

Progress of phase change materials in solar water desalination system: A review

Bing Xu^a, Xiaoguang Zhao^a, Xiaochao Zuo^{b,c,d,*}, Huaming Yang^{a,b,c,d,**}

^a Hunan Key Laboratory of Mineral Materials and Application, School of Minerals Processing and Bioengineering, Central South University, Changsha, 410083, China

^b Engineering Research Center of Nano-Geomaterials of Ministry of Education, China University of Geosciences, Wuhan, 430074, China

^c Laboratory of Advanced Mineral Materials, China University of Geosciences, Wuhan, 430074, China

^d Faculty of Materials Science and Chemistry, China University of Geosciences, Wuhan, 430074, China



ARTICLE INFO

Keywords:

Desalination
Phase change materials
Solar still
Solar interfacial evaporation system

ABSTRACT

Freshwater resources are becoming increasingly scarce. In the context of environmental protection, desalination using solar energy has been one of the most reliable ways to solve the freshwater shortage problem. Solar desalination systems mainly include solar stills and solar interface evaporators, which are driven by solar energy. However, the efficiency of desalination systems is limited by the intermittent and unstable nature of solar radiation. The introduction of phase change materials (PCMs) with latent heat storage capability to overcome the defect has been widely studied. This paper focuses on typical research progress in PCMs integrated solar desalination systems. It analyzes the performance evaluation systems and influence of various factors on the performance of PCMs integrated solar desalination systems. These include the choice of PCMs, the design of the structures and the integration of different systems. Lastly, the challenges faced by integrating PCMs in solar desalination systems are presented, providing references for subsequent researchers.

1. Introduction

In the past few decades, with the increase in population and urbanization, the demand for freshwater resources has been increasing [1]. Moreover, the growing problem of water pollution has led to an extreme shortage of freshwater resources. Compared to freshwater, seawater accounts for about 97.5 % of surface water resources [2]. Therefore, seawater desalination is one of the most reliable methods to solve the shortage of freshwater resources [3]. Desalination technologies are mainly classified into single-phase water treatment and multiphase water treatment. Single-phase water treatment is a desalination process that contains only liquid-phase water, such as electrodialysis and membrane osmosis. Multi-phase water treatment refers to desalination processes contain both liquid-phase and gas-phase water, such as multi-stage flash evaporation and multi-effect distillation [4,5]. The traditional desalination technologies mentioned above have a complex process and consume a lot of fossil energy, which lead to higher costs and environmental pollution problems.

Under the trend of promoting green development, solar desalination

system formed by combining solar energy and desalination technology has become a research craze [6]. In the early days, solar energy was mainly used for distillation, so the solar desalination device was called solar still. In a solar still, seawater is heated and evaporated by sunlight in the evaporation chamber and condensed into fresh water on the inner surface of the glass cover [7–10]. In addition to solar distillers, solar interface evaporators have also become one of the research hotspots for solar desalination systems due to their advantages of safety, low cost, non-pollution, and high freshwater quality. The solar desalination system gets rid of the drawbacks of traditional desalination technology that is overly dependent on fossil energy, and realizes green and sustainable development. Due to the day-night cycle, most solar desalination systems have intermittent operation problems due to limited light hours [11–15]. The system cannot operate continuously and stably, resulting in low efficiency of solar energy utilization. Therefore, it is necessary and urgent to design and develop a new type of solar desalination system to break the limitation of the day-night cycle and realize all-weather solar production of fresh water.

In order to solve the problem of low efficiency of solar desalination systems due to diurnal cycle, phase change energy storage technology as

* Corresponding author. Engineering Research Center of Nano-Geomaterials of Ministry of Education, China University of Geosciences, Wuhan, 430074, China.

** Corresponding author. Hunan Key Laboratory of Mineral Materials and Application, School of Minerals Processing and Bioengineering, Central South University, Changsha, 410083, China.

E-mail addresses: zuoxiaochao@cug.edu.cn (X. Zuo), hm.yang@cug.edu.cn, hmyang@csu.edu.cn (H. Yang).

Nomenclature	
PCM	phase change materials
η_d	solar still energy efficiency
η_{EX}	solar still exergy efficiency
LHTES	latent heat thermal energy storage
CNTs	carbon nanotubes
SSS	stepped solar evaporator
NPCM	nano-particles of phase change material
GO	graphene oxide
SS	solar evaporator
Ag NP	silver nanoparticle
PW	paraffin wax
WLHTESS	without LHTESS
nano-CuO	cupric oxide nanoparticles
nano-Al ₂ O ₃	aluminium oxide nanoparticles
HSD	hemispherical solar desalination
HSDWTR	hemispherical solar desalination with dual reflectors
IC	insulation
CPCM	composite PCM
PVT	Photovoltaic Thermal
HSS	thermal storage system
ETC	solar evaporator with a vacuum tube collector
E _r	evaporation rate
η_s	evaporative efficiency
WHO	World Health Organization
FSPCM	form-stable phase change material
PI	polyimide
PEG	polyethylene glycol
PAA	polyamide acid
MMT	montmorillonite
SA	sodium alginate
CuSAA	CuS agar-based aerogel
MoCCFA	molybdenum carbide/carbon composite of cotton fibers-derived aerogel
BF	bamboo fibers
PVA	polyvinyl alcohol
CB	carbon black
SPCM	solid-solid PCM
MEPCM	magnetic phase-change microcapsules
PEDOT	Poly(ethylenedioxythiophene)
Cppy	carbonized ultralong polypyrrole nanotube aerogels
Cppy-O	octadecane/Cppy spherical evaporator
PNT	polypyrrole impregnated nylon thread
PPy	ultralong polypyrrole nanotube
MCB	modified carbon black
MPCC	magnetic phase-change composites
PDA	Polydiaminopyridine

a new type of renewable energy storage has received more attention. When PCM receives external energy, it stores the energy in the form of latent heat through phase change. The energy is released through the process of reverse phase change when necessary. Researchers have taken advantage of this property of PCMs and applied them to desalination of seawater [16,17]. In a PCM integrated solar desalination system, the PCM stores energy during high daytime light intensities and releases it to continue the desalination process in the evaporation system when light intensities are low or non-existent. It can alleviate the problem of unbalanced energy distribution in space and time, thus increasing the efficiency of solar energy use and freshwater production [18–21]. The different efficiencies of PCMs depending on their location in solar stills have not yet been systematically summarized.

This paper mainly reviews the application of PCMs in solar still and solar interface evaporator. In the solar still, the different performances of different kinds of PCMs in different positions and different structures of the still are described in detail, and the application of PCMs in latent heat recovery of the still is analyzed. The different evaporation characteristics of PCMs in solar interfacial evaporators with gel and micro-capsule structures are analyzed depending on the material and mechanism design. It is hoped that this work will provide a reference idea for subsequent workers studying the application of PCM in solar desalination systems.

2. Application of PCMs in solar still

2.1. Solar still

The solar still is a device that uses solar energy to distill seawater into fresh water. The basic principle of solar stills is to use solar energy to heat seawater in a sealed container to evaporate it. The water vapour condenses on the surface of an inclined glass cover and is discharged into a fresh water collection device [22]. Solar stills are mainly classified into passive and active types. Passive solar stills are desalination units that do not have an electrically driven power element or are actively heated using components such as solar collectors. Its structure is relatively simple and therefore has low performance and efficiency. In order to improve the performance of passive solar stills, active solar stills are

proposed. The active solar still has a higher yield, but due to the complexity and high cost of the process, the passive solar still is still the focus of research [23].

Many researchers have investigated the design of different structures to improve the productivity of passive solar stills. These include double slope solar stills [24], weir type solar stills [25], spherical solar stills [26], solar stills with corrugated and fins [27], and solar stills with flat and convex glass covers tilted at different angles [28], et. all. To further improve the evaporation performance, researchers design of different materials based on structural design. PCMs have been introduced in the stills to increase the energy storage effect. As energy storage materials, PCMs need to absorb energy and store it in a timely manner. Therefore, PCMs are usually placed underneath heat and light conversion materials to form a heat storage layer and wrapped with insulation materials to minimise heat loss. Sharshir et al. [29] added paraffin wax (PW) under the light-absorbing layer of each step as PCM in a weir cascade solar evaporator, and increased the daily production by 31 % as compared to the system without PCM. Shalaby et al. [30] achieved a 12 % increase in productivity in a v-corrugated absorber single-basin solar still by packing the PW into tanks made of galvanised steel and placed below the absorber plate. Theoretical analysis by Mousa and Gujarathi [31] showed that the presence of PCM with a melting point of 40 °C increases the temperature of the distillation cell after sunrise, which ultimately improves the productivity. They also concluded that the selection of PCM with higher melting point (between 40 and 50 °C) is more helpful in increasing the productivity. The addition of PCM to solar stills plays a key role in improving their performance. This section provides an overview of the use of PCM in solar stills.

2.2. Solar still performance evaluation system

To assess the efficiency of solar stills, it is necessary to establish a performance evaluation system. This system can contrast different solar stills and highlight their respective advantages and disadvantages in terms of performance.

2.2.1. Evaporation rate

The evaporation rate is the most direct parameter to assess the per-

formance of a solar evaporator. Under the same conditions, the higher the evaporation rate of the evaporator, the better the performance. The evaporation rate (r_{evap} , $\text{kg} \cdot \text{m}^{-2} \cdot \text{h}^{-1}$) can be calculated by the following formula [32]:

$$r_{evap} = \frac{\Delta m}{S \bullet t} \quad (1)$$

where Δm (kg) is the quality of fresh water produced, S (m^2) stands for the illuminated area of solar still, t (h) is the irradiation time.

2.2.2. Energy efficiency

Applying the principles of the first law of thermodynamics, the thermal behavior of a solar still can be explained through energy efficiency. Solar still efficiency is defined as the ratio between the product of the distillate yield per unit area along a day and the sum of the solar energy intensities per unit area during the day in latent heat at the average pool water temperature [33]. This can be expressed by the following equation:

$$\eta = \frac{\sum_{i=1}^{t=t} \Delta m \times h_{fg}}{S \times \sum_{i=1}^{t=t} I_{(t)} \times 3600} \quad (2)$$

where Δm is the hourly yield in kg, h_{fg} is the latent heat of evaporation in J/kg, S is the surface area of the basin, $I_{(t)}$ is the hourly intensity of solar radiation in W/m^2 . The i is the parameter of time. Since energy efficiency represents the efficiency of a complete run of a still, the upper limit of i , represents the length of a complete run of a still. Therefore, t varies from distiller to distiller for different complete operating times. Theoretically, t can be infinite, but from a practical point of view, the evaporation efficiency of a still is usually calculated by letting it work only for a day or a few days.

2.2.3. Exergy efficiency

On the other hand, exergy studies originating from the second law of thermodynamics can be used to assess the maximum input energy that can be extracted from the absorbed energy. This concept is closely related to energy quality. Exergy is a property associated with a system and its environment, which is influenced by the state of both the system and the environment. The efficiency of a process based on the second law of thermodynamics is determined by minimizing the wastage and degradation of available work from a given input of available work.

For solar still, the exergy efficiency is calculated from Refs. [34,35]:

$$\eta_{Ex} = \frac{\text{Solar Still Output Exergy}}{\text{Solar Still Input Exergy}} = \frac{Ex_{Evap}}{Ex_{Input}} \quad (3)$$

The exergetic production of a solar still can be expressed in terms of the amount produced per hour [36]:

$$Ex_{Evap} = \left(\frac{\Delta m \times h_{fg}}{3600} \right) \times \left(1 - \frac{T_a + 273}{T_w + 273} \right) \quad (4)$$

where Δm is the water output of the solar distiller per hour (kg), h_{fg} is the latent heat of evaporation (J/kg). T_a the ambient temperature in ($^{\circ}\text{C}$), and T_w water in ($^{\circ}\text{C}$).

While, the exergetic input to a solar still from solar irradiance can be quantified as Ex_{Input} and this value is derived using a specific equation [37]:

$$Ex_{Input} = Ex_{sun} (\text{For solar still}) = S \times I(t)_s \times \left\{ 1 - \left[\frac{4}{3} \times \left(\frac{T_a + 273}{T_s} \right) \right] + \left[\frac{1}{3} \times \left(\frac{T_a + 273}{T_s} \right)^4 \right] \right\} \quad (5)$$

where S is the effective area of the basin in the solar still in m^2 , $I(t)_s$ is the amount of incident solar irradiation in W/m^2 on solar static tilted glass, and T_s represents the temperature of the sun, taken as 6000 K.

2.3. Different distributions of PCMs in solar still

PCMs can be distributed in different locations in a solar still: below the evaporator basin and in the PCM tank alone. This subsection focuses on the effects of different structure types and material designs on the performance of solar stills with PCMs located in different locations.

2.3.1. PCMs below the basin

When the PCM is located below the basin, the simplest construction is the conventional type. Conventional type of retort involves laying the PCM flat underneath the light absorbing layer, on the bottom of the retort basin to form a heat storage unit of a specific thickness. In the study by Asbik et al. [38], they used sand and PW as sensible and latent heat storage materials in a solar still, respectively. The experimental setup is shown in Fig. 1a, where item 4 represents the PCM layer.

Fig. 1b-d illustrate the hourly and daily freshwater production of the distiller using air, sand, and PW as thermal storage materials, respectively. Fig. 1b is the control group. The comparison shows that the freshwater production capacity of the control group was significantly lower than the other two groups, with a daily production of only $1.13 \text{ kg}/\text{m}^2$. The distillers using sand and PW had daily production rates of $3.79 \text{ kg}/\text{m}^2$ and $4.08 \text{ kg}/\text{m}^2$, respectively, which were 235.39 % and 261.06 % higher than that of the control group. Fig. 1e&f shows the transient and overall thermal efficiency of the distiller in decibels, respectively. The solar still with storage media (sand and PW) had better transient thermal efficiency compared to the control group. Moreover, the overall thermal efficiencies of the three groups were 16.01 %, 40.25 % and 50.88 % respectively. In comparison with the control group, the overall thermal efficiency of the solar still with sand and PW storage media increased by 152.80 % and 223.09 %, respectively. The inclusion of PCM not only enhances the freshwater yield of the still but also reduces energy waste.

The above PCM evaporator is the simplest structure. In addition, there are many studies to further improve the performance of the evaporator through structural adjustments and the use of different PCMs. Kateshia et al. [39] developed a new type of solar still using aluminum pin fins and palmitic acid as a composite PCM laid flat at the bottom of the still basin. Where the palmitic acid was used as PCM and aluminium pin fins were used to increase the thermal conductivity of PCM. Fig. 2 shows the schematic diagram of the experimental setup, and three types of solar stills were designed for performance analysis. Fig. 2a shows a solar distiller with a PCM, Case II; Fig. 2b shows a solar distiller with a PCM and needle fins, Case III; along with a blank control group, Case I. Fig. 2c shows the cumulative freshwater yields throughout the day for the three cases. The cumulative yields (L/m^2) for Case I, Case II, and Case III were 3.8, 4.9, and 5.4, respectively. The total cumulative production rates for Case II and Case III were 24 % and 30 % higher, respectively, compared to the distiller without PCM (Case I). In addition, the production rate of Case III was increased by 8 % compared to Case II. This suggests that the incorporation of aluminum needle fins in PCM integrated solar stills can further enhance the performance and efficiency of the stills.

As shown in Fig. 2e, Kabeel et al. [40] combined PW and parabolic solar concentrator into a conventional solar evaporator to form a new type of distillation apparatus. Where PW acts as a PCM, the parabolic solar concentrator enhances the absorption of solar radiation in the distillation basin. The researchers found that this modified still equipped with PCM and solar concentrator achieved an average daily cumulative freshwater production rate of about $7.2 \text{ L}/\text{m}^2$. This is a significant improvement of about 55 %–65 % compared to conventional stills. In the conventional type of solar stills, the PCM is laid flat at the bottom of the still and the presence of PCM significantly improves the evaporation performance of the still.

Another type of distiller is the step distiller. Unlike conventional stills, the PCM in a step still is distributed in a stepped pattern, but it is still located below the light-absorbing layer. Each step has a weir that

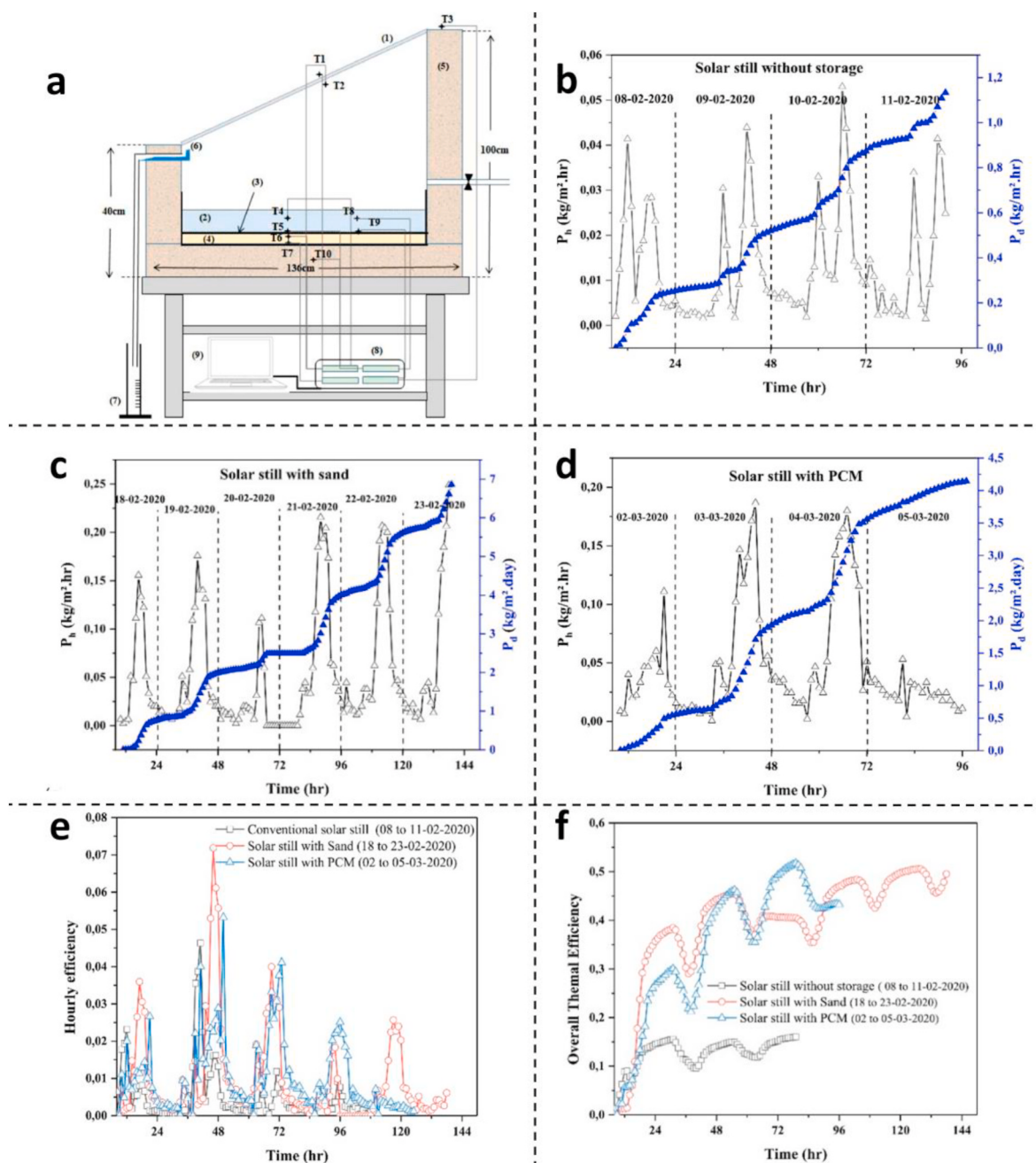


Fig. 1. (a) Illustrative diagram of the experimental setup components: (1) Glass cover, (2) Brackish water, (3) Absorber, (4) Storage material, (5) Thermal insulation, (6) Condensed water collector, (7) Distillate measuring tube, (8) Data logger, (9) Laptop computer; (b) variations of hourly and daily freshwater productivity for solar still without storage (air); (c) variations of hourly and daily freshwater productivity for solar still with sand; (d) variations of hourly and daily freshwater productivity for solar still with PCM; instantaneous (e) and overall thermal efficiencies (f) of solar still with sand, PCM and without storage [38].

gives the seawater a longer retention time. In addition, a thin layer of water exists on the evaporation surface, which helps to promote channel formation.

Two cascade solar stills with and without latent heat thermal energy storage system (LHTES) were built by Tabrizi et al. [25], respectively. The performance of the two evaporators was compared under identical conditions. In the evaporator with LHTES, PW was used as PCM. The structure of the cascade solar still is shown schematically in Fig. 3a, where each step includes a weir to control the flow of water and increase the residence time. This design also helps to reduce the problem of trenching that is common in inclined solar distillation chambers. Fig. 3b depicts the hourly productivity of the still with and without LHTES on a cloudy day. It can be seen that the total productivity of the still with

LHTES was 3.4 kg/m² per day, while the total productivity of the still without LHTES was 2.1 kg/m² per day. This indicates that even in the stepped solar still, the presence of PCM can still significantly improve the evaporation efficiency of the solar still.

PW is used as a PCM and has a low thermal conductivity. The low thermal conductivity is not conducive to the timely transfer of heat. The researchers found that adding nanoparticles to PW enhances its thermal conductivity but reduces thermal stability [41–46]. There have been researchers using CNTs [47], graphene oxide [42], zinc oxide [48], copper oxide [49], cerium oxide [50], aluminum oxide [51] and titanium oxide [52] to improve the thermal conductivity and thermal stability of PW. Adibi Toosi et al. [53] designed and constructed a novel stepped solar evaporator (SSS) as shown in Fig. 3c. PW was still chosen

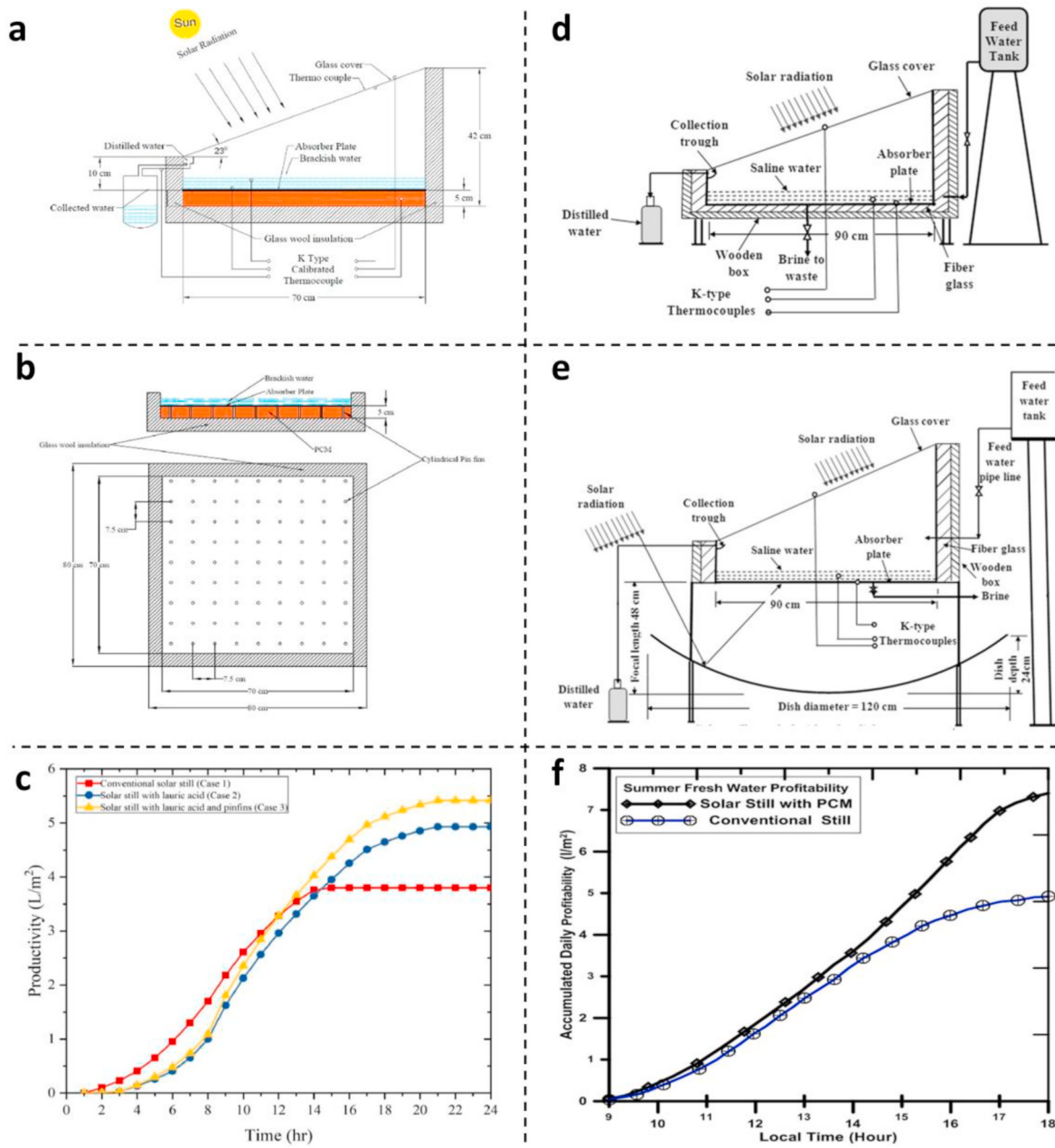


Fig. 2. The details of the experimental setup (a) solar still with PCM reservoir (Case II); (b) the details of absorber solar still with PCM reservoir and pin fins (Case III); (c) the accumulated freshwater productivity the whole day for the three cases [39]; (d&e) schematic diagram of the conventional solar still and a solar still incorporated with solar concentrator and PCM in basin; (f) average daily accumulated freshwater profitability for solar still with PCM and parabolic solar concentrator [40].

as the PCM, and adding graphene oxide (GO) and Fe_3O_4 to PW to form hybrid nanoparticles of phase change materials (NPCM). The SSS consists of three absorbing stages and one evaporating stage to prevent complete saturation of the device space. In order to increase the daily production rate, the SSS was tested and optimized in four different states: state I simple SSS, state II SSS with the addition of PCMs, state III SSS with the addition of hybrid NPCM, and state IV SSS with the addition of hybrid NPCM under magnetic field. Fig. 3d illustrates the production of the SSS in various modes throughout the day rate versus time. By adding PCM to the rectangular chambers under each order, the production rate of the SSS was increased by 37 % over the simple SSS. By using a hybrid NPCM, the production rate was increased by 75 %, while using a hybrid NPCM in the presence of a magnetic field, the production rate of the simple solar static system (SSS) was increased by 98 %. To

address the low thermal conductivity of PW, GO was used to enhance the thermal conductivity of PW. As a result, the high thermal conductivity of the hybrid NPCM improves the distillation rate of the solar still. Another nanomaterial in the hybridized NPCM is Fe_3O_4 , which has a significant effect under magnetic field and improves the distillation of SSS.

Sathyamurthy [54] prepared composite PCM by doping silver nanoparticles in the PW. From the experimental results, it was found that doping 2 % silver nanoparticles in PW can increase the thermal conductivity by 1.25 times. As shown in Fig. 3e, Sathyamurthy placed the PCM in a stepped solar distiller. Three sets of solar stills were designed, namely (i) without PCM, (ii) with PW, and (iii) with PW-doped Ag nanoparticles. For case i, the cavity between the absorber and the base of the distiller was filled with sawdust as an insulating material; for cases ii and iii, the cavity was filled with PW and PW doped with Ag

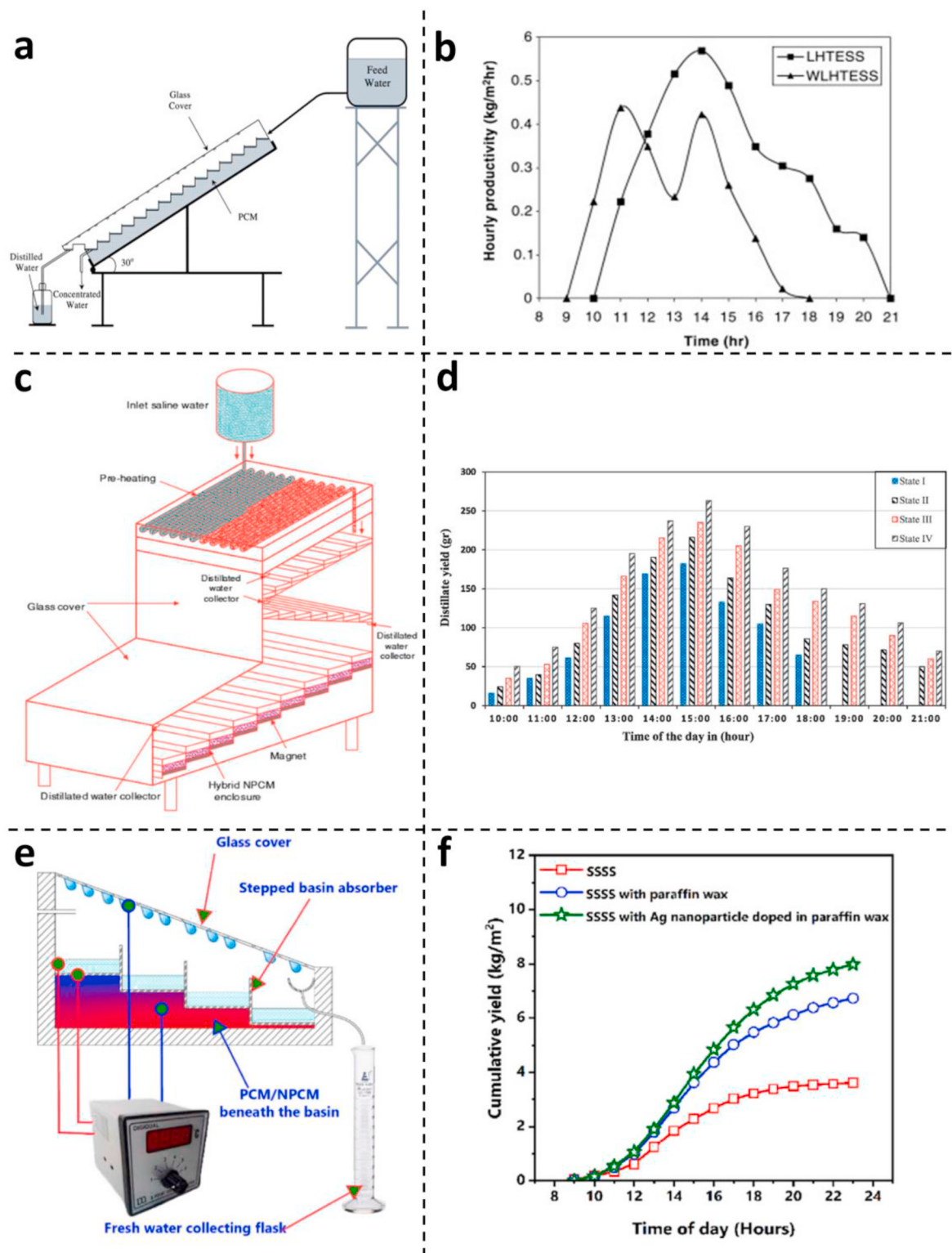


Fig. 3. (a) Cross sectional view of a schematic diagram of cascade solar still; (b) variations of hourly productivity with time for still with LHTESS and without LHTESS (WLHTESS) in typical cloudy day [25]; (c) schematic of new designed SSS integrated with evaporator part and NPCM; (d) daily production of the SSS for different experimental states [53]; (e) schematic of the basin of stepped SS; (f) cumulative palatable water yield from the stepped basin SS, SS with PW and SSS with Ag nanoparticle doped in PW as thermal energy storage [54].

nano particles. Fig. 3f is the cumulative palatable water yield from the stepped basin SS, SS with PW and SSS with Ag nanoparticle doped in PW as thermal energy storage. The cumulative palatable water yield by the step still without PCM was low (3.61 kg/m^2) and the cumulative fresh water volume of the still containing PW was increased by about 46.29 %

(6.73 kg/m^2). The addition of Ag NP to PW increased the cumulative freshwater yield by 54.67 % and 15.59 % compared to SS without PW and SS with PW only. Ag NP caused the PW to exhibit higher thermal stability and higher evaporation rate, which resulted in a substantial increase in the freshwater yield of the still.

In addition to the above types, researchers have innovated many other structures of solar stills based on the use of PCMs. The effect of parameters such as absorption area, water depth, water temperature and evaporation area on the productivity of solar stills was considered. Researchers have used corrugated absorbers to maximize the absorption area, still placing the PCMs below the absorber [55,56]. Compared to flat solar stills (Fig. 4a), Abdullah et al. [56] designed a convex solar evaporator (SS) with PW and Ag nanoparticles as a composite PCM as shown in Fig. 4b. Convex SS achieves increased evaporation area, minimized water thickness, avoidance of dry spots and reduced heat capacity through the use of raised receiving surfaces and core absorbing materials. Fig. 4c compares the capacity of convex SS and conventional solar still. It can be observed that the difference in productivity between the two types of solar stills increases with time and reaches its maximum value around 14:00 due to the presence of the composite PCM and the convex absorbing surface. The daily water production of the convex SS is 7200 ml/m² per day, while the daily water production of the conventional solar still is 3400 ml/m² per day, which is an increase of about 112 % in the daily water production of the convex solar still. The

incorporation of composite PCM and the design of the convex absorption surface significantly improve the performance of the evaporator.

Afrand et al. [57] studied the effect of external reflector on the performance of solar evaporator. Maiti [58] found that external reflector can increase the productivity by 240 %. External reflectors are used to amplify the solar radiation entering the system. And if the system includes internal reflectors, it will redirect the radiation to the water, effectively reducing the heat loss from the side walls [59]. Additionally, although many kinds of PCMs are available for desalination systems in the operating temperature range, most of them have poor thermal conductivity. With the development of nanotechnology, nanomaterials with high thermal conductivity have been widely used. The thermal conductivity of PCMs can be greatly enhanced by mixing the nano-thermally conductive materials with PCMs to form composite PCMs. Shoeibi et al. [60] achieved 45 % yield enhancement by adding nano-CuO to PW. Shoeibi et al. [61] compared nano-CuO with nano-Al₂O₃ and found that the nano-CuO was more effective in enhancing the performance of the evaporator.

Based on the above study, Sathish et al. [62] designed a

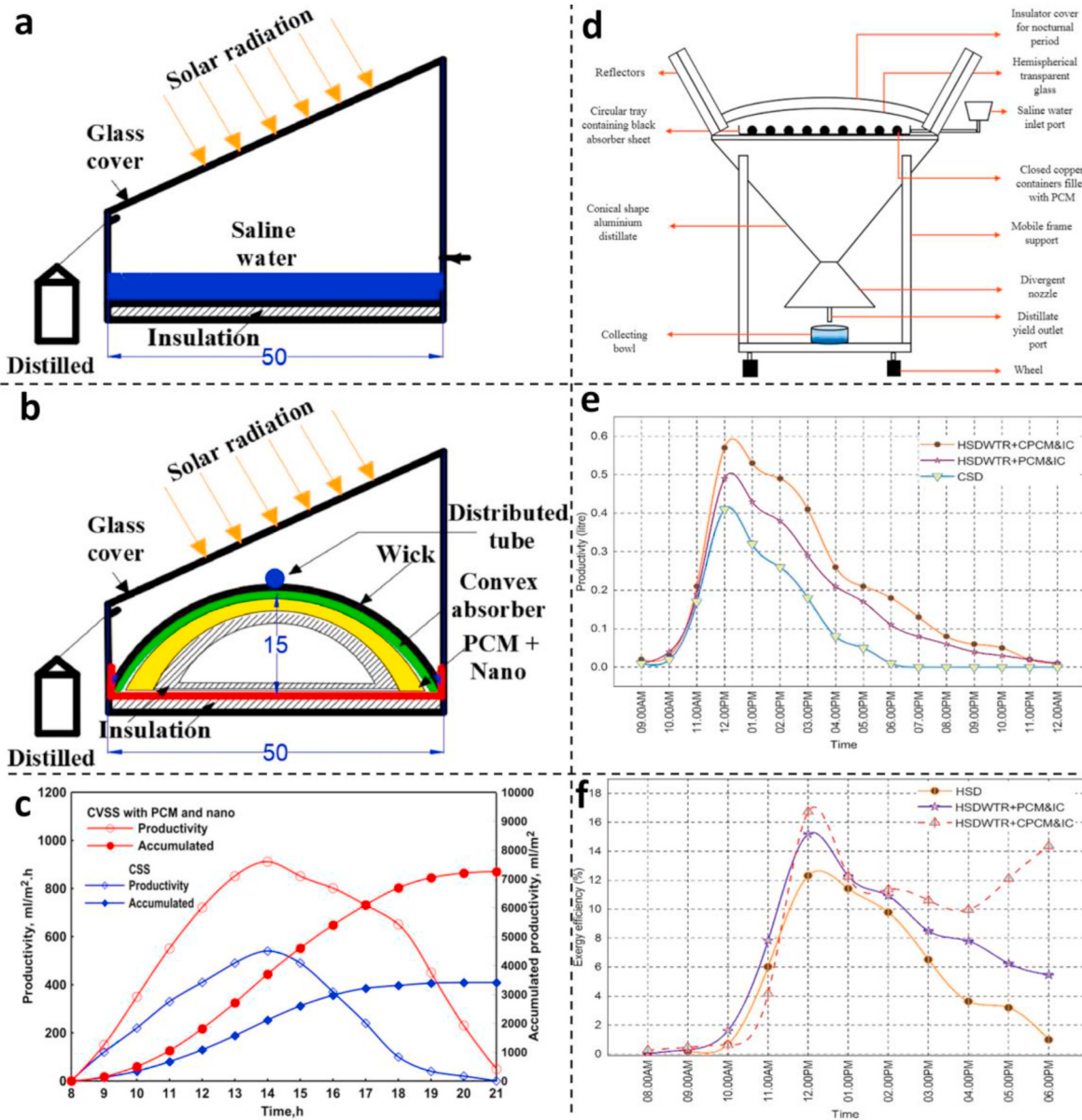


Fig. 4. Schematic of conventional (a) and convex (b) solar stills; (c) hourly and cumulative productivity for convex and conventional SSs [56]; (d) schematic view of the hemispherical desalination unit; comparison of the hourly distillate (e) and exergy efficiency (f) of HSD, HSDWTR + PCM&IC, and HSDWTR + CPCM&IC [62].

hemispherical solar distiller as shown in Fig. 4d. The device includes external double reflector and a composite PCM with PW and aluminium powder. Three cases of solar distillation systems were studied. Case I: Hemispherical system without reflector, utilizing only PCM and insulation (HSD). Case II: Hemispherical system equipped with dual reflectors, utilizing pure PCM and insulation (HSDWTR + PCM&IC). Case III: Hemispherical system featuring dual reflectors, utilizing composite PCM and insulation (HSDWTR + CPCM&IC). Fig. 4e compares the hourly freshwater production for the three scenarios and finds that the evaporator containing a composite PCM as well as a dual reflector produces more freshwater. Fig. 4f compares the hourly thermal efficiencies for the three cases and finds that all systems show an increasing trend before noon. The thermal efficiency of the conventional system drops significantly after 16:00 due to insufficient light, while the improved system continues to produce fresh water. The thermal efficiency of Case II becomes negligible after 18:00, while Case III exhibits higher efficiency during this time due to the addition of aluminium powder to the PW.

The productivity of solar stills is affected by several variables, including design, climate, and operational variables [63,64]. Based on the addition of PCMs, the performance of a solar still can be enhanced by integrating it with other systems to form a composite structure, such as using a solar water heater [65], a blower [66], a water circulation system [67], a hot air injection system [68], or solar dishes [69]. Wang et al. [70] developed a novel solar dehumidification air conditioning system, using RT-44 as an organic PCM, with a humidification-dehumidification desalination unit. The innovation of this device is the use of PCM and a photovoltaic/thermal solar pre-heating device. The air is preheated before it enters the dehumidifying rotor. In addition, the solar system was modified by using PCM to meet the heating requirements of the air conditioning system at night. The results showed that the Photovoltaic Thermal (PVT) system was used to generate electricity and heat, and the electricity generated was used for the dehumidification fan and auxiliary heater. The use of the PCM

resulted in significant savings in input thermal energy. For most of the day, the temperature of the discharge water from the energy storage tank was consistently higher than that of the input air from the reheat section of the air cooling system. Integration of PCM, the solar dehumidification air conditioning system and the humidification and dehumidification desalination unit further enhances the performance of the still.

In addition, Shehata et al. [71] developed a solar evaporator with an ultrasonic humidifier, PW as the PCM and vacuum collector as shown in Fig. 5a. The ultrasonic humidifier was used to enhance the rate of water evaporation from the water basin. The vacuum collector provides heat to the solar evaporator. PCM was used to store energy. Four different cases (PCM; PCM and ultrasonic humidifier; PCM and vacuum solar collector; PCM and ultrasonic humidifier combined with vacuum tube solar collector) were designed. The daily freshwater production of the evaporator with different embedded components was examined using a conventional evaporator as a blank control group. Fig. 5 b&c shows the hourly and cumulative water production of the five different evaporators. Case 5 was observed to have the highest hourly freshwater production capacity and cumulative yield by integrating the ultrasonic humidifier, vacuum solar collector and PCM. In addition, the integration of the ultrasonic humidifier with the vacuum solar collector produced a substantial impact, especially by increasing the evaporation rate, vapour pressure.

Table 1 summarizes the performance of the different structural designs of solar stills described above based on PCM. Most of the solar still systems choose PW as the PCM, and nanoparticles are also added to the PCM to form a composite PCM. Compared to conventional stills, the addition of PCM and the design of the structure can also greatly improve the evaporation performance of the stills. When the distiller system is integrated with other systems, the evaporation performance is increased more obviously.

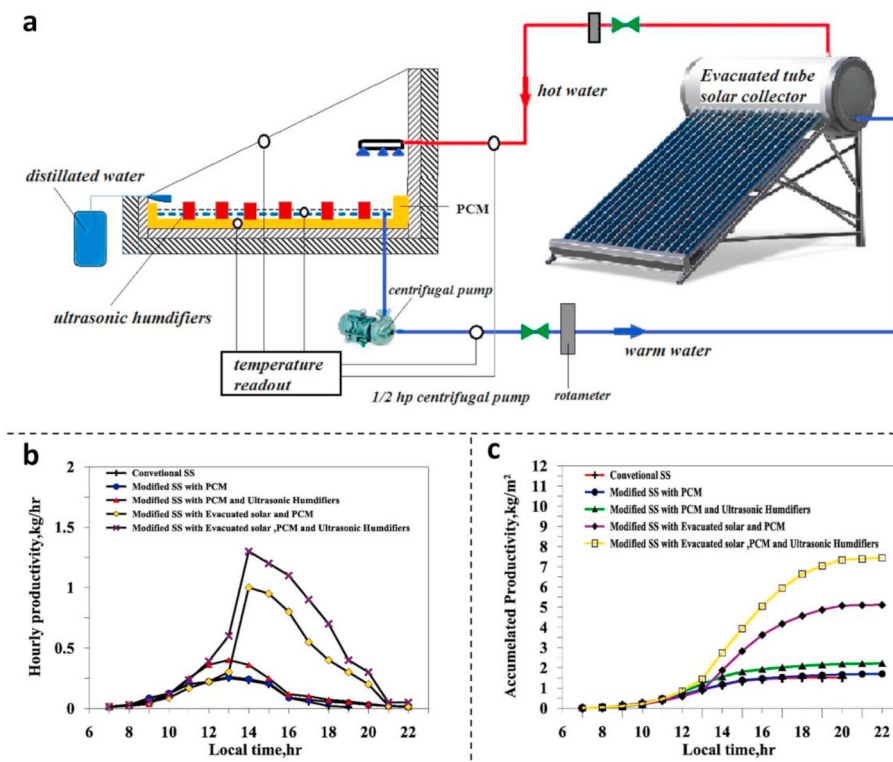


Fig. 5. (a) Schematic diagram for the proposed solar still; (b) hourly productivity of freshwater for five different solar still cases; (c) accumulated production of the freshwater for five different cases [71].

Table 1

Performance of solar stills with different structural designs.

Type of still	PCM	Daily productivity ($\text{kg}\cdot\text{m}^{-2}$)	Energy Efficiency (%)	Exergy Efficiency (%)	Ref.
Conventional	PW	4.08			[38]
Aluminium pin fins	Palmitic acid	5.40	57 %	5.54 %	[39]
Parabolic concentrator	PW	7.20	\	39.5 %	[40]
Weir-type	PW	5.14	\	\	[25]
Stepped-type	PW	1.79	\	\	[53]
Stepped-type	PW with Ag NP	7.98	\	\	[54]
Convex shape absorber	PW with Ag	7.20	\	\	[56]
Dual reflectors	PW with Al	\	7.5 %	17 %	[62]
Humidification-dehumidification	RT-44	81.85	\	\	[70]
Ultrasonic humidifier	PW	7.40	\	\	[71]

2.3.2. PCMs encapsulation inside the basin

In the PCM described above the evaporator located at the bottom of the basin may result in significant dissipation of stored energy to the enclosure. Despite the provision of insulation, the potential for heat loss to the surrounding ambient air is high. Therefore, the encapsulation of

PCMs in the still type has been the subject of many studies.

Vigneswaran et al. [44] filled concentric tubes with PCMs of different phase change temperatures. The experimental findings showed that, compared to PCM-1 alone, PCM-2 together enhanced the freshwater yield of the still by 8.6 %. PW was put inside a tube-shaped still by

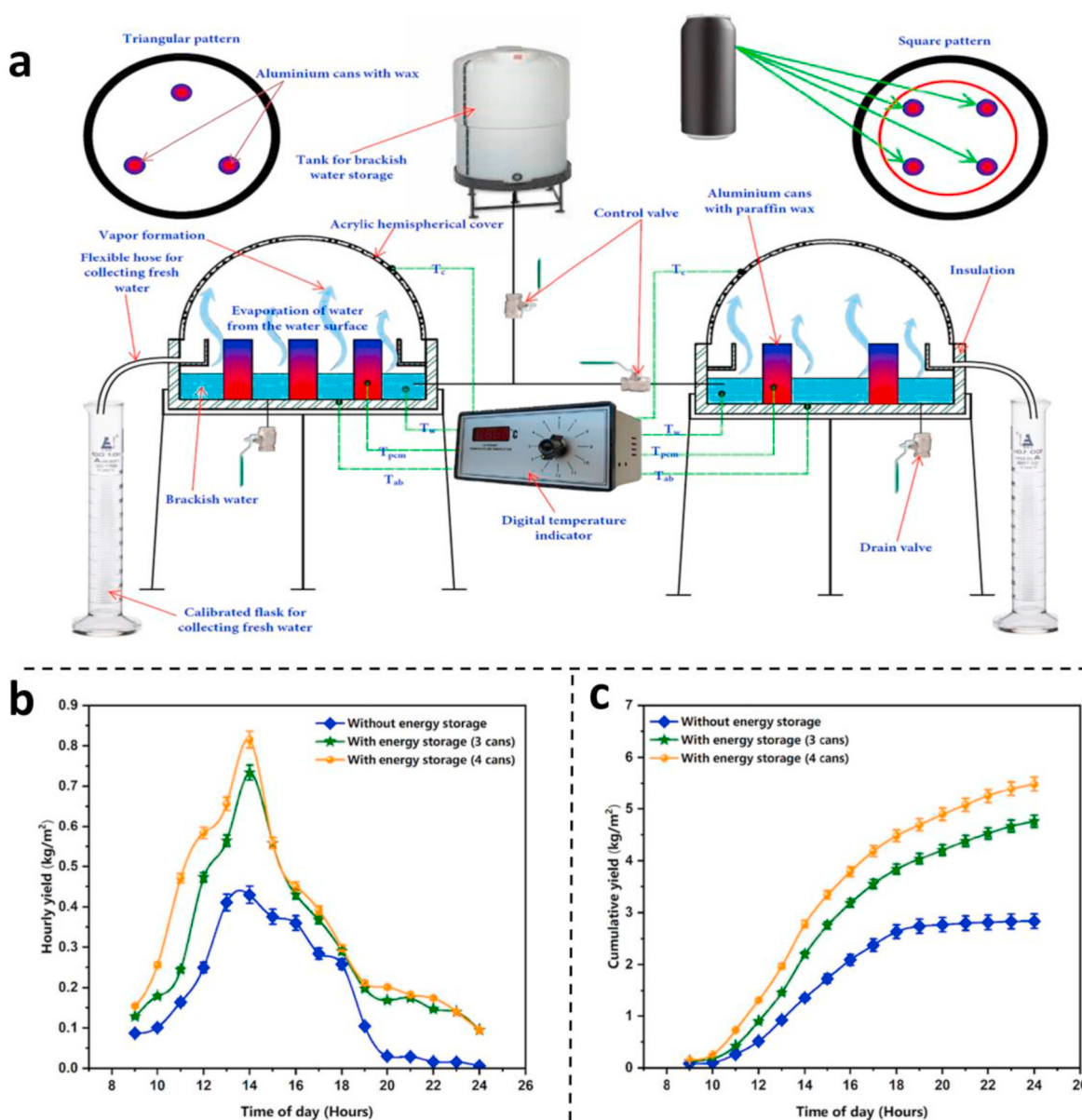


Fig. 6. (a) Graphical representation of HSS with triangular and square pattern of PCM encapsulation; (b) hourly variations on potable water from three different configurations; (c) hourly variations on cumulative yield from three different configurations [76].

Thakur et al. [72]. In comparison to the bottom still, the results revealed a 42.4 % increase in freshwater productivity. Metal encapsulation of PCM in distillers has been studied extensively, such as copper balls with PCM by Arunkumar et al. [73], petroleum jelly filled container tubes by Ho et al. [74], and fabricated aluminum tubes with PCM by Elashmawy et al. [75]. However, these distillers are more expensive, which eventually raises the price per liter of pure water.

To address the above problem, Kannan et al. [76] encapsulated PW as PCM in clean waste aluminum cans as an energy storage system for hemispherical solar evaporator. As shown in Fig. 6a, the aluminum tanks were arranged in two ways, square and triangular, to assess their effect on the water production potential of the still. Fig. 6 b&c shows the hourly and cumulative daily water production by the thermal storage system (HSS) in the aluminum tanks with and without PCM during the experiment. The maximum water production for the HSS, 3-can (arranged in a triangular pattern) and 4-can (arranged in a square pattern) were 0.42 kg/m^2 , 0.73 kg/m^2 and 0.81 kg/m^2 at 14:00 h. Obviously, the higher PCM mass in the square-patterned encapsulated cans allows for more energy storage and leads to higher production rates. The cumulative water production of the conventional HSS reached 2.92 kg/m^2 . But the incorporation of three and four phase change canisters resulted in a significant increase in the cumulative water production to 67.12 % and 92.80 %, respectively. The increase in potable water productivity of the HSS with PCM is mainly attributed to the higher water temperatures achieved with the PCM-equipped tanks. The PCM exhibits excellent energy storage potential, leading to faster evaporation and higher productivity.

Kaabinejadian et al. [77] conducted a study on solar assisted hybrid

desalination system. As shown in Fig. 7, the system consists of a trough concentrating solar collector, a heating and thermal storage unit and a desalination unit. The solar collector provides the required input energy to the system. The heat storage and thermal storage unit includes a latent heat storage tank and an auxiliary boiler. The latent heat storage tank is a shell-and-tube latent heat energy storage device [78], and the selection of the PCM with the appropriate melting point is crucial to its performance [79]. Five different eutectic PCMs ($\text{NaNO}_2/\text{NaOH}$, $\text{LiNO}_3/\text{NaCl}$, $\text{NaCl}/\text{NaNO}_3$, $\text{NaNO}_3/\text{KNO}_3$ and KOH/LiOH) were studied within the temperature range applicable for solar energy systems [77]. The total cost ratio and thermal efficiency of the system when using different PCMs were analyzed. The thermal efficiency of the system was found to be significantly improved by using a PCM with a higher melting point. By selecting a PCM with a melting point close to the setting value of the auxiliary boiler, the need for significant fuel combustion can be reduced, thus increasing the thermal efficiency. The fifth PCM (KOH/LiOH) had the greatest impact on thermal efficiency, increasing from 0.06 % to 0.28 %. This significant effect is also reflected in the change in the total cost share, which decreases from $8.35/\text{s}$ to $0.63/\text{s}$ in winter.

2.4. PCMs in latent heat recovery

One of the main disadvantages of solar stills is the waste of energy. The vapour liquefies on the upper glass during the operation of the still and the heat released is usually transferred to the environment outside the still. Researchers have noticed this flaw in solar stills and conducted studies on it. Madhlopa et al. [80] evaluated the performance of a three-stage externally cooled solar concentrator using numerical

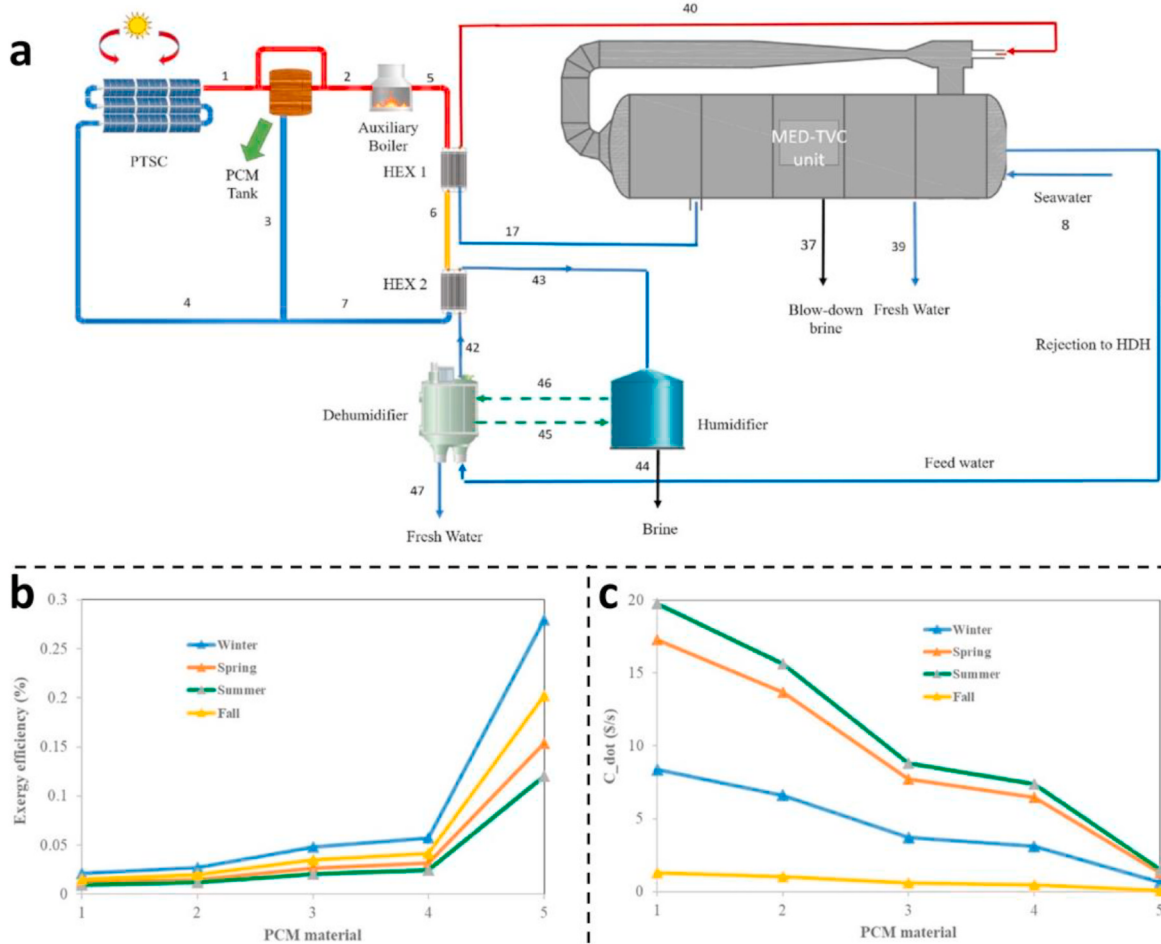


Fig. 7. (a) Schematic of the proposed system; average seasonal variation of exergy efficiency (b) and total cost rate (c) with alteration of PCM materials [77].

methods. The heat loss in all stages of the condenser was successfully prevented by efficiently transferring the heat generated during the distillation process to the water basin above. As a result, the performance of the system was improved by 62 % compared to a simple solar distiller. Monowe et al. [81] theoretically studied the preheating effect of an internal fan in the evaporator chamber for transferring liquid. The evaporator chamber is equipped with a fan that facilitates the transfer of the generated steam to an external condenser. This condenser is responsible for extracting the internal heat of the steam and transferring it to a secondary fluid. This secondary fluid can then be stored and utilized for household consumption or to enhance the system's performance during periods without sunlight. By employing this setup, the system's efficiency can be enhanced to 77 % and 85 % in the respective scenarios. Shafii et al. [82] achieved 52 % efficiency by recovering the latent heat of distillation using a thermoelectric module.

Currently, PCM is able to store a small fraction of the sun's radiant energy during the day in a solar still. This stored energy can be subsequently released at night to facilitate the desalination process. However, due to the absorption of solar radiant energy by the PCM during the day, this leads to a decrease in productivity. To address this problem, Faegh et al. [83] designed a novel solar evaporator using PW as PCM. It prevents the seawater from coming in contact with the PCM and uses all the radiant energy during the day to evaporate the seawater. In this evaporator, the PCM is filled in an external condenser. During the day, the

vapour from solar radiation is directed to the external condenser filled with PCM for condensation. The PCM absorbs and stores the waste heat from the condenser. Thus, energy storage within the PCM occurs solely through the vapour within the PCM and its subsequent condensation. It should be noted that solar energy is not stored directly in the PCM. The stills are also equipped with heat pipes and vacuum tubes. In order to investigate the performance of the modified stills, four different stills were designed as shown in Fig. 8a. In Test 1, a solar evaporator with a vacuum tube collector (ETC) was used. Test 4 examined the combined effects of glazing insulation and a storage system utilizing external latent heat. This particular system is known as the insulated cover glass system and includes an external condenser fitted with a PCM. Fig. 8b shows the operation of the system in Test 4 during the day and night. In this process, the vapour generated in the basin is transported to an external condenser, which is filled with PW. This transport is achieved by means of a fan, which transfers heat to the condenser. All the heat released by the condensation of the vapour is stored in the PW. During the night, the heat stored inside the PW is transferred to the upper tank via heat pipes. This heat transfer enables the desalination process to continue. Fig. 8c depicts the variation of solar radiation intensity and water production with time in test 4. The maximum water production of $1.05 \text{ kg/m}^2 \text{ h}$ occurs at 14:00, with a slight delay of 30 min compared to the peak solar intensity of 970 W/m^2 reached at 13:30. This delay is attributed to the high thermal mass of the system. In addition, the incorporation of the

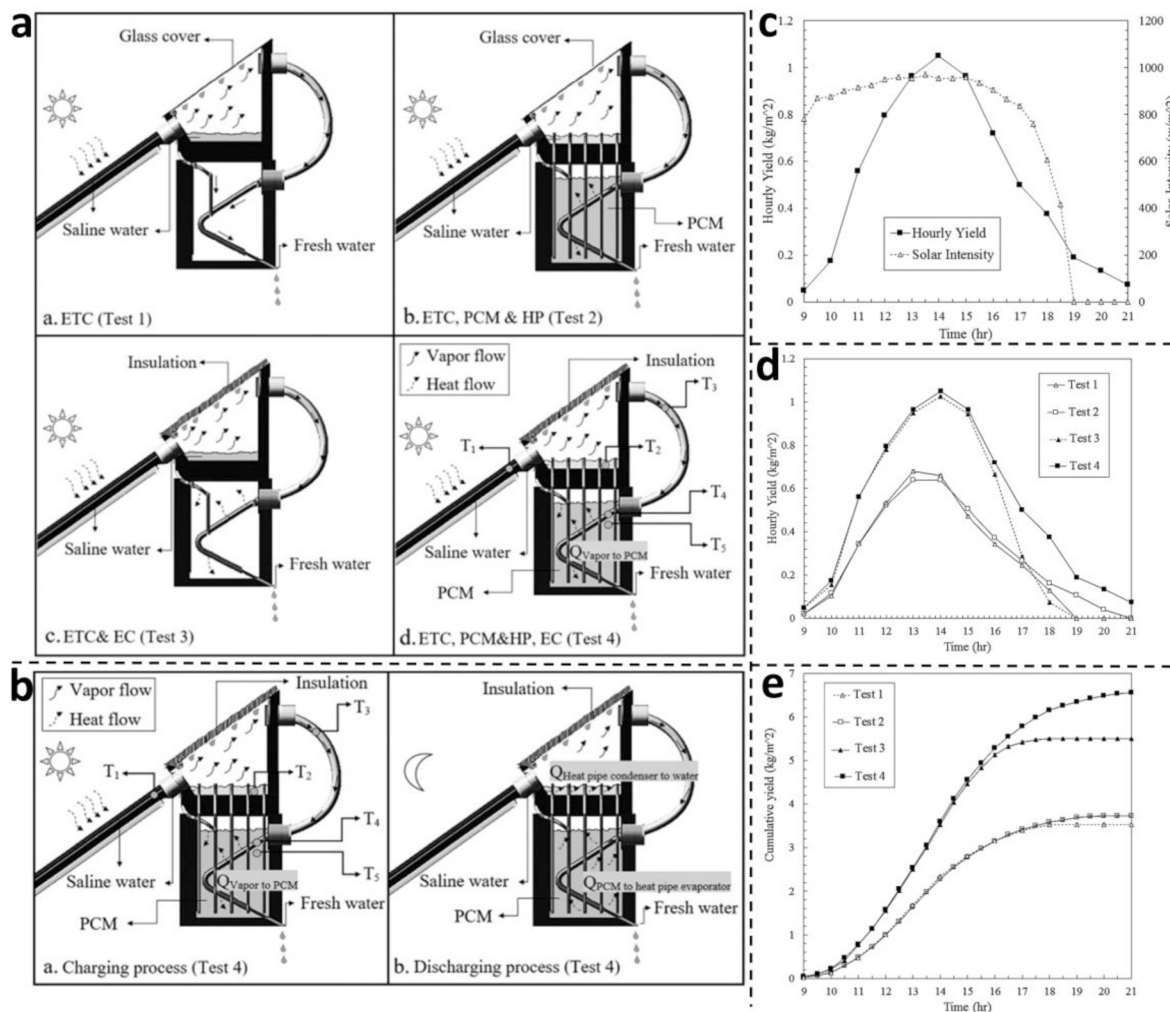


Fig. 8. (a) Schematic of the tests conducted; (b) schematic of the processes in the system with external condenser containing PCM and heat pipes (Test 4), charging process and discharging process; (c) hourly water yield and solar intensity for the system with latent heat storage system (external condenser filled with PCM) (Test 4); (d) hourly water yield for different tests; (e) cumulative water yield for different tests [83].

PCM allowed the water production to continue for 2 h after sunset, until 21:00. This extended production cycle was achieved due to the LHTES system.

Fig. 8d depicts the water production rates of four experiments at different times. Test 1 is consisted of a unit consisting of a water basin and a vacuum tube collector. In this configuration, the vapour formed inside the system condenses on the glass cover. As a result, the maximum water yield achieved is $0.68 \text{ kg/m}^2 \text{ h}$. Test 2 is similar to test 1 with the addition of a thermal storage system containing PW. However, due to the condensation of some of the vapour on the glass cover, the heat recovered from distillation was lower, resulting in similar yields between Test 1 and Test 2. The presence of the thermal storage system in Test 2 resulted in only a small increase in yield after 17:00. In Test 3, the glass cover was insulated, resulting in all vapour condensing in an external condenser without PCM. In comparison with Test 1, Test 3 revealed that although the input radiation was reduced, the water production increased significantly up to 1.025 kg/m^2 due to the insulation of the glass cover. In Test 4, the external condenser used in Test 3 was filled with PW as a PCM. In this way, the addition of the heat storage system in Test 3 allowed most of the latent heat of evaporation to be stored and the desalination continued until 21:00. **Fig. 8e** shows the cumulative water production for the four experiments. The results showed that the highest water yield was achieved by the Test 4 system with an external PCM condenser. This was followed by Test 3, Test 2, and finally Test 1. It is noteworthy that the system incorporating external latent heat storage (Test 4) showed an impressive 86 % increase in yield compared to the simple solar still (Test 1).

The study by Faegh et al. [83] demonstrates the feasibility of PCM and heat pipes in recovering and storing latent heat from water vapour. By utilizing the stored heat, continuous water production was achieved even at night. As a result, the daily production increased significantly. The addition of an external condenser and insulated solar glass increased water production by 56 % without the use of PCM. When using an external condenser filled with PCM, the water yield was increased by 86 %. It shows important implications for the heat recovery of distillers to improve their performance.

The study of solar stills is important for desalination of seawater using solar energy as a power source. Conventional solar stills rely heavily on sunlight and can only produce fresh water when sunlight is abundant. However, they cannot operate stably under conditions of weak or lack of sunlight, limiting their efficiency in producing fresh water. By integrating PCM into solar stills, the cyclical nature of solar energy can be addressed. PCM have the ability to store excess heat from sunlight and release it when sunlight is weak. This means that in a solar still, the PCM can effectively utilize the heat energy accumulated during the day for continuous desalination at night. The integration of the PCM improves the efficiency of solar energy utilization and increases the yield of fresh water in the solar system.

In solar stills, there are various forms of PCMs used. Different positions of PCMs in the still, different types of PCMs, different compositional structures of the stills and their integration with other systems all have a significant impact on the performance of solar stills. Among many PCMs, PW stands out as the most widely used PCMs due to its high energy storage capacity, stable physicochemical properties, and wide range of melting points, etc. In addition, some organic and inorganic PCMs have also been used, such as palmitic acid, RT-44, $\text{NaNO}_2/\text{NaOH}$, $\text{LiNO}_3/\text{NaCl}$, etc. The use of PCMs enhances both the overall yield and energy utilization of the solar still. Nanoparticles are added to the PCM to enhance its thermal conductivity and improve the thermal storage performance of the distillers. In addition, the implementation of PCMs in the solar still allows the recovery of latent heat during the evaporation process. The use of this PCM improves the overall energy utilization efficiency of the solar stills, thus improving their performance. The research on PCMs is crucial for the development of solar stills. The integration of PCM in solar stills brings it closer to commercialization and has great potential to address the shortage of fresh water in certain

regions.

3. Application of PCMs in sustainable solar interfacial evaporation system

3.1. Solar interfacial evaporation system

In a solar still, the photo-thermal conversion material and the PCMs are placed at the bottom of the evaporator. Desalination is achieved by heating the water at the bottom. The evaporator system requires excellent light absorption, efficient photothermal conversion, fast vapour transfer and low heat loss to achieve high evaporation rate [84–86]. In the evaporator system described above, the separation between photothermal conversion and water evaporation leads to higher heat losses. This results in lower heat utilization of the evaporator system. To solve this problem, solar interfacial evaporation systems have received much attention.

Solar interfacial evaporation systems work similarly to solar evaporators. Both convert solar energy into thermal energy to heat seawater for evaporative desalination. However, in the interfacial evaporation system, both photothermal conversion and water evaporation occur at the water-air interface. Solar energy is used exclusively to heat the water at this interface, effectively integrating photothermal conversion and water evaporation. As a result, this integration minimizes heat loss and significantly improves energy efficiency.

Since the first solar interfacial evaporator was designed in 2014 [87], material innovation [88,89] and thermal management [90,91] have been the key to improve the evaporation performance of interfacial evaporators. Currently, solar interfacial evaporators are mainly available in aerogel and microcapsule structures [92–95]. Both work on the same principle of using photothermal conversion materials at the interface to convert solar energy into thermal energy to heat seawater and make it evaporate. Currently, the evaporation efficiency of most interfacial evaporators can exceed 80 % [96], and some research groups have even observed evaporation efficiencies exceeding 100 % [97]. The highest evaporation rate can reach $10.9 \text{ kg/(m}^2\text{-h)}$ [98]. Compared with solar evaporators, solar interfacial evaporator systems have significant advantages in terms of energy utilization and productivity.

Although solar interfacial evaporators generally outperform solar stills, they are still subject to the intermittent nature of solar energy. This makes solar interfacial evaporators less efficient and limits their desalination capacity. To solve this problem, many researchers have combined PCM with solar interfacial evaporation systems to overcome the intermittent nature of solar radiation and to achieve high evaporator efficiency [99–101]. Latent heat gels and phase change microcapsules can be formed by combining PCM with gels and microcapsules in solar interfacial evaporation systems. This section summarizes and outlines the research on latent heat gels and phase change microcapsules.

3.2. Performance evaluation system of solar interfacial evaporation system

3.2.1. Evaporation rate

The evaporation rate is the rate at which water is converted from a liquid to a gaseous state during the desalination process. It is an important performance index of the evaporator. The evaporation rate (r_{evap} , $\text{kg}\cdot\text{m}^{-2} \text{ h}^{-1}$) can be calculated by the following equation:

$$r_{evap} = \frac{\Delta m}{S \times t} \quad (6)$$

where Δm (kg) is the mass loss of water, S (m^2) is the illuminated area of the evaporator, t (h) is the illumination time.

3.2.2. Evaporation efficiency

The evaporative efficiency η_s is the proportion of solar energy used

for water evaporation and can be calculated using the following equation [102]:

$$\eta_s (\%) = \frac{r_{evap} \cdot \Delta H_w}{I_R} \times 100\% \quad (7)$$

where r_{evap} represents the rate of evaporation, ΔH_w is the total evaporating enthalpy of pure water (2400 kJ kg^{-2}), and I_R is the irradiance intensity.

3.2.3. Solar photothermal conversion efficiency

Photothermal conversion efficiency measures how effectively solar

energy is converted into thermal energy. It is usually expressed as a percentage of the solar energy absorbed in an interfacial evaporation system that is successfully converted into useable thermal energy. A higher thermal conversion rate is directly related to a higher efficiency of energy utilization within the system. The solar thermal conversion efficiency (η) can be calculated using the following equation [103]:

$$\eta = \frac{\Delta H_m \cdot w}{(t_{end} - t_{onset}) \cdot P \cdot S} \quad (8)$$

where ΔH_m is the melting enthalpy of the gas aerogel/PCM composite, w is the weight of the gas aerogel/PCM composite, t_{onset} and t_{end} represent

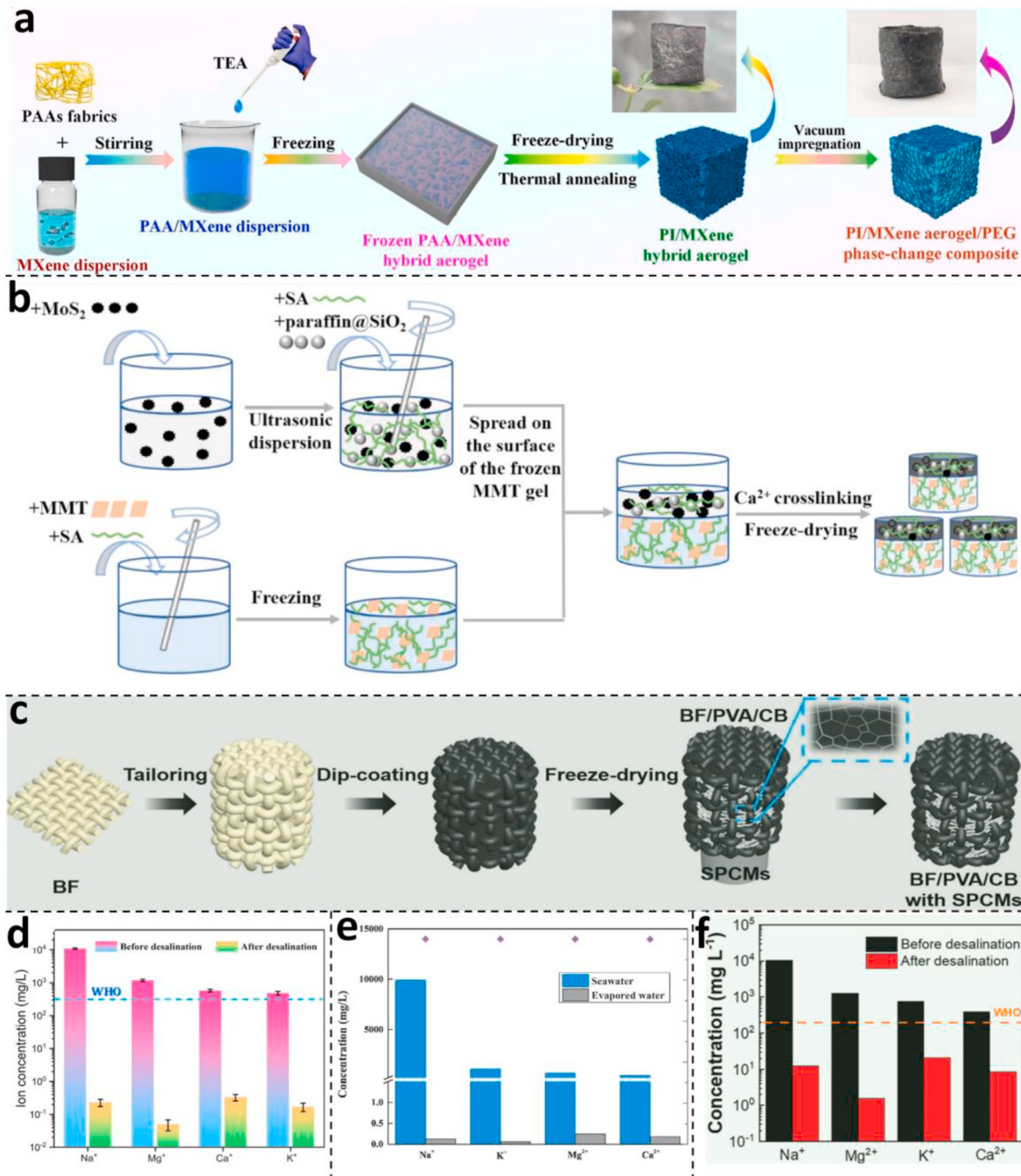


Fig. 9. (a) Schemes for the fabrication routes of PI/MXene hybrid aerogels and their composites with PEG [106]; (b) schematic diagram of preparation of MoS₂/MMT latent heat bilayer aerogels [107]; (c) schematic of preparation of 3D BF/PVA/CB with SPCMs [109]; (d) ion concentrations of real seawater and its desalinated water [106]; (e) salt ion concentration and salt ion removal rate before and after seawater desalination [107]; (f) primary ions in a simulated seawater sample before and after desalination [109].

the start and end time of the sunlight-driven melting phase change of the PCM loaded in the composite, P is the radiation intensity, and S is the irradiation area.

3.2.4. Salt ion filtration efficiency

In solar interfacial evaporators, the salt ion filtration efficiency refers to the effectiveness of removing salt ions from the fresh water obtained by evaporating seawater. A higher salt ion filtration efficiency means that more salt ions are effectively removed from the water, leading to a reduction in the salinity of the water.

The main concern is the concentration of Na^+ , K^+ , Mg^{2+} , and Ca^{2+} in the water. The higher the salt ion filtration efficiency of the interface evaporator, the lower the salt ion concentration in the desalinated water obtained. When the salt ion level in the desalinated water is below the WHO standard of 200 mg/L, it signifies that the evaporator has achieved outstanding performance in seawater desalination.

3.3. Aerogel-based composite PCMs for solar-driven seawater interfacial evaporation

Liquid PCM is prone to leakage when the PCM absorbs energy and undergoes a phase transition. There is a volume difference before and after the phase transition [101,104]. To solve this problem, researchers have developed sophisticated methods to cope with it. This part focuses on one of these approaches, the PCM-integrated aerogel-structured solar interfacial evaporator. Aerogel is a nanoscale porous solid substance formed by replacing the liquid phase in a gel with a gas. It has significantly high porosity, low density, high specific surface area and high pore volume ratio. The unique properties of aerogel can provide substantial mechanical support to the PCM. This ensures its shape stability and prevents leakage of the PCM in the molten state [105].

Solar interfacial evaporators with integrated PCMs have three main components: frame support structure, photothermal conversion material, and energy storage material. In addition, some evaporators have thermal insulation materials, water transport materials, etc [87]. The performance of the solar interfacial evaportaors was largely determined by the structural combinations and material designs. A comparative analysis of some representative solar interface evaporators with PCM-integrated gel structures is presented below.

Zheng et al. [106] developed a novel composite form-stable phase change material (FSPCM) consisting of a hybrid aerogel of polyimide (PI) and MXene, along with polyethylene glycol (PEG) as the PCM. As shown in Fig. 9a, the researchers used a combination of freeze-drying and thermimide chemical techniques to prepare PI/MXene hybrid aerogels by varying the weight ratio of MXene nanosheets to polyamide acid (PAA). The use of MXene nanosheets as an effective solar energy absorber not only greatly improved the photothermal conversion efficiency of the PI/MXene/PEG composite FSPCM, but also increased the bulk capacity of the hybrid aerogels. Then the PI/MXene/PEG composite FSPCM with different MXene nanosheet contents were prepared by vacuum impregnation. The photothermal conversion efficiency of the PI/MXene/PEG composite FSPCM reached 87.28 % when the loading of MXene was 20 wt%. When compared to the control group, the device equipped with the hybrid composite FSPCM demonstrated a significant improvement in the evaporation rate, measuring $1.24 \text{ kg m}^{-2} \text{ h}^{-1}$, and an evaporation efficiency of 50.6 %. This is due to the fact that MXene nanosheets effectively absorb sunlight and convert it into heat. In addition, the still devices with PI/MXene/PEG composite FSPCM exhibited some water evaporation after the solar irradiation ceased. This was due to the latent heat energy released from the PEG within the aerogel system, which caused the water to continue to evaporate. Resulting in a higher evaporation quality compared to the control. Based on the data in Fig. 9d, the concentrations of salt ions such as K^+ , Ca^{2+} , Na^+ , and Mg^{2+} in water before and after the evaporation process were determined. Before evaporation, the concentration of these ions in seawater was high. However, after desalination using the hybrid

aerogel/PEG composite, the ion concentrations decreased significantly, with all values falling below 0.33 mg L⁻¹. This is well below the drinking water standards set by the WHO.

The aforementioned PI/MXene/PEG composite FSPCM showed some improvement in the performance of photothermal conversion and water evaporation compared to the normal blank control group. However, the relevant performance is still low, especially the evaporation efficiency, which is only 50.60 %. Moreover, this type of evaporator is a single-layer structure, and the heat stored in the PCM is conducted to the lower water layer, resulting in heat loss. In order to further improve the performance of the solar interface evaporator, a double-layer structure solar interface evaporator was developed by Guo et al. [107]. The upper layer of the evaporator was made up of MoS_2 and PW@ SiO_2 aerogel phase-change microcapsules. The lower layer consisted of montmorillonite (MMT) aerogel. As shown in Fig. 9b, MMT was first dispersed in water and sodium alginate (SA) was added to form a gel. Then frozen it to form the lower layer MMT aerogel. The MMT aerogel exhibits a vertically porous structure with relatively regular sheet-like arrangements. This unique structure reduces the distance water needs to travel compared to a disordered porous structure, enabling a more stable water supply to the evaporation interface. In addition, due to the naturally low thermal conductivity of MMT, it can reduce heat conduction loss and act as an insulation layer. Nano-flower-shaped MoS_2 was dispersed in deionized water, SA was added to form a MoS_2 gel, and then PW@ SiO_2 phase change microcapsules were added to obtain a MoS_2 latent heat gel. The obtained MoS_2 latent heat gel was then cryogenically crystallized and laid on the surface of the MMT aerogel, and the resulting double-layer aerogel was soaked in a 3 wt% calcium chloride ethanol solution for complete cross-linking. Finally, heating was applied to remove the ethanol and obtain the desired MoS_2 - PW@ SiO_2 /MMT double-layer aerogel.

MoS_2 acts as a photothermal conversion material, absorbing solar energy and converting it into heat. PW, as a PCM, serves as an energy storage medium. The SiO_2 outer shell of PW provides protection to prevent it leakage during the metling process. The upper layer of the designed aerogel demonstrates an impressive light absorption rate of 88 %. On the other hand, the thermal conductivity of the lower layer made of MMT aerogel is $0.43 \text{ W m}^{-1} \text{ K}^{-1}$, which is lower than that of pure water ($0.6 \text{ W m}^{-1} \text{ K}^{-1}$). The high light absorption and low thermal conductivity are important factors for achieving high efficiency of photothermal conversion and reducing heat loss. The evaporation rate of MoS_2 /MMT latent heat aerogel is $1.30 \text{ kg m}^{-2} \text{ h}^{-1}$, under the sunlight condition, and the evaporation rate still reaches $0.72 \text{ kg m}^{-2} \text{ h}^{-1}$ within 20 min after stopping the sunlight condition, which is about 1.9 times of that of the unadded PCM aerogel. The evaporation efficiency was 86.22 %, which was much higher than that of the still assembled with PI/MXene/PEG composite FSPCM mentioned above. The desalination performance of the MoS_2 /MMT latent heat aerogel is showcased in Fig. 9e. The concentrations of K^+ , Ca^{2+} , Na^+ , and Mg^{2+} in seawater were markedly reduced to 0.06, 0.18, 0.13, and 0.24 mg/L, respectively, resulting in a removal rate of salt ions exceeding 99.90 %. The concentration of salt ions in the desalinated water was found to be significantly lower than the standard set by the WHO.

A similar double-layer aerogel structure designed by Yu et al. [108] through using molten salts as the PCM, using agar gel as the backbone, and embedding the CuS superstructure with strong light absorption and heat conversion ability into the agar gel backbone to form the upper aerogel layer. The lower layer of the aerogel consists of molybdenum carbide-coated waste cotton fiber-based aerogel. This aerogel exhibited not only efficient water transport capability, but also excellent thermal insulation properties. In addition, low-temperature PCMs are used to enhance the ability of the solar interface evaporator to overcome the intermittent nature of solar energy. This enables the storage and subsequent reuse of solar energy. As indicated in Table 2, the dual-layer CuSAA/MoCCFA aerogel design achieves an impressive light-to-heat conversion efficiency of 92.77 % under 1 sun illumination. It also

Table 2

Performance of solar interface evaporators based on latent heat gel structures with different design materials.

Materials	Thermal conversion efficiency (%)	Eva-rate ($\text{kg}\cdot\text{m}^{-2}\cdot\text{h}^{-1}$)	Eva-efficiency (%)	Ref.
PI/MXene/ PEG	87.28 %	1.24	50.60 %	[106]
MoS ₂ - PF@SiO ₂ / MMT	88.00 %	1.32	86.22 %	[107]
CuSAA/ MoCCFA	92.77 %	2.44	\	[108]
BF/PVA/CB with SPCM	\	3.80	151.00 %	[109]

shows a water evaporation rate of $2.44 \text{ kg m}^{-2} \text{ h}^{-1}$ and a remarkable salt ion removal rate of 99.97 %.

However, most bulky 3D solar vaporizers are easily damaged and not portable. To address this issue, Liang et al. [109] have designed a flexible and robust 3D hydrogel/fiber evaporator. As shown in Fig. 9c, bamboo fibers (BFs) were first cut and used as the framework of the entire evaporator, providing support. Then a polyvinyl alcohol/carbon black hydrogel (PVA/CB) was coated onto the BF as a photo-thermal conversion material, forming an outer hydrogel/fiber framework (BF/PVA/CB). To prevent the leakage of the liquid PCM, which can occur when PW is used as PCM, a solid-solid PCM (SPCM) with high thermal conductivity composed of graphene and PW is selected as the medium for thermal storage and conduction in this evaporator. The SPCM is inserted into the BF/PVA/CB to construct a 3D hydrogel/fiber evaporator, namely BF/PVA/CB with SPCM. This evaporator incorporates hydrogel, which significantly enhances the flexibility of the fibers. The presence of hydrogel within the fibers helps distribute stress, while the fibers themselves provide positive reinforcement to the hydrogel, ultimately improving the mechanical strength of the entire evaporator. This makes the 3D BF/PVA/CB with SPCM highly mechanically durable, capable of maintaining its integrity and stable evaporative performance even after rigorous transportation and storage.

Incorporation of solar selective spectral conversion material (SPCM) and 3D BF/PVA/CB in the evaporator reduces the enthalpy of evaporation of the hydrogel, leading to a significant increase in the evaporation rate. Under illumination conditions, the 3D BF/PVA/CB with SPCM achieves an impressive evaporative rate of $3.80 \text{ kg m}^{-2} \text{ h}^{-1}$, representing a remarkable 109 % increase compared to the standard BF/PVA/CB evaporative rate. The evaporative efficiency is as high as 151 %. Even in the absence of light, 3D BF/PVA/CB with SPCM can achieve an evaporative rate of $0.31 \text{ kg m}^{-2} \text{ h}^{-1}$, which is approximately 1.4 times that of ordinary BF/PVA/CB. Fig. 9f shows the partial ion concentration changes in simulated seawater samples before and after desalination. The concentrations of K⁺, Ca²⁺, Na⁺ and Mg²⁺ decreased to 21.15, 8.4, 12.65, and 1.55 mg/L. They were much lower than those in seawater, which met the drinking water standards set by the WHO. In addition, no salt crystals were observed at the top and both sides of the evaporator after a long desalination operation. It was shown that the prepared 3D BF/PVA/CB of SPCM effectively resisted salt clogging and had excellent water transfer performance. Compared with the aforementioned evaporators, the 3D BF/PVA/CB with SPCM has higher evaporation performance, as well as higher mechanical strength and excellent portability.

This section summarized and analyzed the PCM-integrated gel-structured solar evaporator. The aerogel mainly acts as a scaffold to provide support for the whole evaporator. The incorporation of PCM as an energy storage unit helps to overcome the intermittent nature of the solar radiation and thus enhances the evaporation performance of the solar interfacial evaporator to a certain extent. The selections of different gel structures, photothermal conversion materials, and PCMs have a significant effect on the performance of the solar interfacial

evaporator. Table 2 summarizes some performance parameters of the evaporators designed with four different gel structures and materials mentioned above. In comparison, the 3D BF/PVA/CB with SPCM exhibits higher evaporation rate and efficiency. This work will also provide insights for scholars studying PCM-integrated gel-structured solar evaporators, allowing for further development in this field.

3.4. Microencapsulation-based composite PCMs for solar-driven seawater interfacial evaporation

To solve the leakage problem of PCM during solid-liquid phase change, another approach is to encapsulate the PCM inside compact inorganic walls using encapsulation techniques, such as SiO₂ [110], TiO₂ [111], CaCO₃ [112], Fe₃O₄, and others. Unlike the gel method, this method completely encapsulates the PCM in a dense inorganic shell to form phase change microcapsules. The dense shell effectively prevents the internal PCM from leaking during the melting process. It also allows external heat transfer to the internal PCM for latent heat storage. These microcapsules act as energy storage units in the solar interface evaporator. However, the prepared phase change microcapsules do not have photothermal conversion capability. Researchers have found that it is possible to add photothermal conversion materials, such as metal oxide materials [113], biomass materials [114], and carbon-based materials [115], to the shell of phase change microcapsules. In this way, the phase change microcapsules can have a high photothermal conversion capacity and achieve efficient photothermal conversion [116]. And let the converted thermal energy be absorbed by seawater and PCM in the form of sensible and latent heat. This effectively improves the efficiency of solar energy utilization.

Based on the above methods, the PCM integrated microencapsulated solar evaporator consists of three main parts. The inorganic dense shell layer serves as the support body of the evaporator to prevent PCM leakage. The internal PCM acts as a heat storage unit. The photothermal conversion material is applied to the outer surface of the shell, which serves to absorb the sunlight and convert it into heat energy. Based on this principle, Shen et al. [117] designed a MoS₂-decorated magnetic phase-change microcapsules (MoS₂-MEPCM), as shown in Fig. 10a. N-docosane was used as the PCM, which was encapsulated in a Fe₃O₄/SiO₂ composite shell to form Fe₃O₄/SiO₂@n-docosane magnetic phase-change microcapsules (Fe₃O₄/SiO₂-MEPCM). By doping Fe₃O₄ nanoparticles in the silica shell, the microcapsules acquired a magnetic effect, enhanced separability from the salt crystals, and improved long-term evaporation performance. Subsequently, the PEDOT functional layer was coated on the surface of the Fe₃O₄/SiO₂-MEPCM composite by interfacial oxidative polymerization. Finally, MoS₂ nanosheets were assembled on the microcapsule surface by electrostatic adsorption to obtain MoS₂-MEPCM.

PEDOT has strong light absorption in the wavelength range of 900–2000 nm [118]. The narrow bandgap of MoS₂ nanosheets provides spectrally tunable and efficient broadband light absorption [119]. Therefore, combining PEDOT with MoS₂ nanosheets can achieve up to 96.86 % photothermal conversion efficiency. In the MoS₂-MEPCM system, an aerogel felt with low thermal conductivity is used as an insulation layer. This layer effectively concentrates the heat at the evaporator-water interface. And a water pump with excellent hydrophilic properties is used to transport the water to the evaporator interface. The evaporation rate of MoS₂-MEPCM was $2.06 \text{ kg m}^{-2} \text{ h}^{-1}$ at a light intensity of 1.0 kW m^{-2} . Compared to the evaporator without PCM, the mass of evaporated water increased by 0.33 kg m^{-2} when the evaporator was exposed to a light intensity of 1.0 kW m^{-2} for 110 min and then to dark condition for 110 min. MoS₂-MEPCM showed an evaporation efficiency of 95.30 % at a light intensity of 1.0 kW m^{-2} . Moreover, the efficiency of the evaporator increased with increasing light intensity. At a light intensity of 3.0 kW m^{-2} , the efficiency of the evaporator reached 96.69 %. The concentration of salt ions in the desalinated water was significantly reduced and complied with the

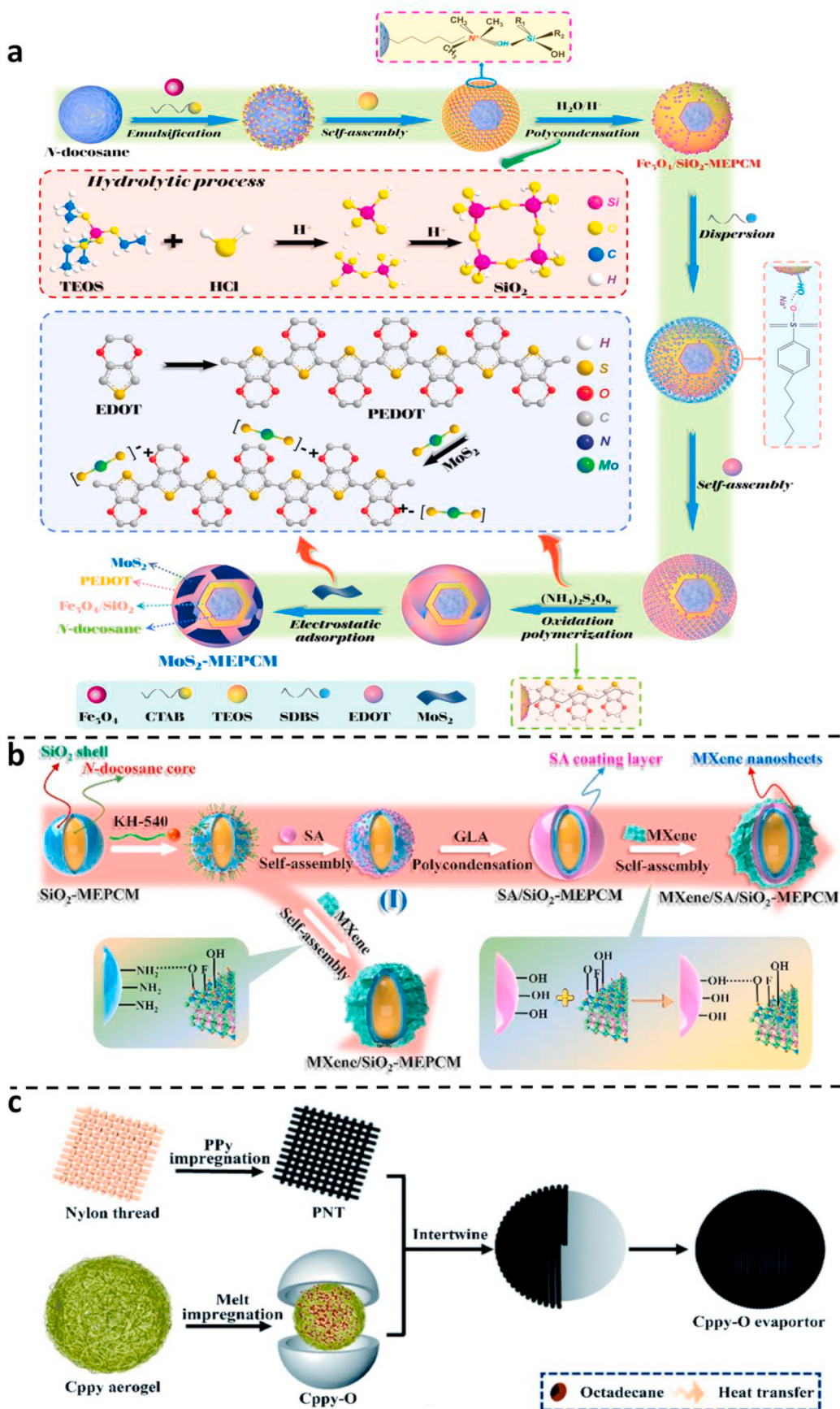


Fig. 10. (a) Synthesis strategy and reaction mechanism of MoS₂-decorated magnetic phase-change microcapsules [117]; (b) synthesis strategy and reaction mechanism of MXene/SA/SiO₂-MEPCM [121]; (c) the preparation procedures of the Cppy-O evaporator [124].

drinking water standards set by the WHO.

Compared with MoS₂, MXene has received more attention due to its excellent properties, including high solar-to-thermal conversion efficiency in the visible and near-infrared regions, significant specific surface area, excellent thermal conductivity, and abundant hydrophilic functional groups [120]. Zhang et al. [121] used MXene modification and SA to coat the phase change microcapsules to obtain MXene/SA-/SiO₂-MEPCM. Similar to the previously mentioned MoS₂-MEPCM, n-docosane and SiO₂ were selected as the PCM and the inorganic shells, and the emulsion interfacial condensation method was used to synthesize the phase change microcapsules (SiO₂-MEPCM), as shown in Fig. 10b. SA was encapsulated on the surface of SiO₂-MEPCM by interfacial self-assembly to obtain SA/SiO₂-MEPCM. SA is a polymer with a surface rich in hydroxyl and carboxyl groups, which exhibits excellent wetting properties due to its high hydrophilicity and biocompatibility. The incorporation of SA enhances the evaporation performance of the evaporator and contributes to its overall efficiency [122]. MXene nanosheets are firmly attached to the SA/SiO₂-MEPCM surface through hydrogen bonding interactions. Combining SA and MXene nanosheets in an innovative manner endows the phase change microcapsules with an excellent photothermal conversion efficiency of 97.00 % and exhibits excellent wetting properties.

By using peleith as an insulating material, heat is concentrated at the interface between the evaporator and water, reducing heat loss. The water conveyor can continuously transport seawater to the surface of the evaporator for a stable water supply. In this study, the prepared MXene/SA/SiO₂-MEPCM achieved an evaporation rate of 2.11 kg m⁻² h⁻¹ under one-sun illumination. The total water production of MXene/SA/SiO₂-MEPCM increased by 1.01 kg m⁻² on partly cloudy days. Compared to the control evaporator, the evaporator with MEPCM achieved an evaporation efficiency of 80.88 %, which was significantly higher than that of the evaporator without MXene or PCM. The concentrations of four typical ions (K⁺, Ca²⁺, Na⁺, and Mg²⁺) in the condensate desalinated on the basis of MXene/SA/SiO₂-MEPCM were reduced to 0.044, 0.385, 0.113 and 0.023 mg/L, respectively, which are well below the WHO drinking water standards. The removal of heavy metal ions such as Cr³⁺, Cd²⁺, Cu²⁺, and Pb²⁺, as well as organic dyes including methyl orange and methyl blue by this evaporator exceeded 99.9 % [123]. Therefore, this evaporator can not only desalinate seawater but also treat wastewater and industrial effluents, contributing to environmental protection.

Both of these microcapsule-structured solar evaporators use n-dodecane as the PCM and MoS₂ and MXene as the photothermal conversion materials. However, Geng et al. [124] designed a spherical evaporator (Cppy-O) as shown in Fig. 10c. Octadecane was injected into the Cppy aerogel to form a Cppy-O composite PCM. The Cppy-O composite PCM was then placed into a spherical container and securely wrapped with nylon thread impregnated with polypyrrole (PNT) to form the Cppy-O evaporator. Cppy has a three-dimensional network structure and a porous structure in which capillary forces encapsulate the octadecane melt in the aerogel. This prevents the PCM leakage and provides good shape stability. Cppy also has an extremely high loading capacity (1500 %). It can load large amounts of octadecane and rapidly transfer and store the converted solar energy into the octadecane. PNT acts as both a photo-thermal conversion material and a water transport layer covered with rough PPY nanoparticles. These nanoparticles enhance light absorption, and PNT also has excellent superhydrophilicity and rapid water transport, wetting with water within 1.4 s. At a solar irradiance of 1.0 kW m⁻², the evaporation rate of the Cppy-O evaporator reached 2.62 kg m⁻² h⁻¹, which was higher than that of the hollow spherical evaporator (2.24 kg m⁻² h⁻¹) and the pure octadecane spherical evaporator (2.26 kg m⁻² h⁻¹). The evaporation efficiency of the Cppy-O evaporator was 92.7 %, which was also higher than that of the pure octadecane spherical evaporator (79.9 %) and hollow sphere evaporator (79.2 %). After long-term operation, there was no obvious salt deposition on the surface of the Cppy-O evaporator, indicating its strong salt resistance. In addition, the desalination capacity of the

evaporator was simulated and evaluated. The results showed that the concentrations of the four salt ions K⁺, Ca²⁺, Na⁺, and Mg²⁺ in the water were significantly reduced from the initial 10000 mg/L, 6969 mg/L, 395 mg/L, and 400 mg/L to 1.12 mg/L, 0.56 mg/L, 0.43 mg/L, and 1.24 mg/L, with a removal rate of nearly 100 %, which demonstrated the high removal efficiency of the evaporator.

Li et all [95], encapsulated n-docosane with a SiO₂/Fe₃O₄ composite shell, achieved a higher evaporation rate of 2.67 kg m⁻² h⁻¹. The SiO₂/Fe₃O₄ composite shell prevents PCM from leaking during the phase transition. And the Fe₃O₄ nanoparticles can make the phase change microcapsules obtain magnetic response, which is good for recycling. The composite phase change microcapsules MCB-MPCC were obtained by modifying PDA and MCB nanoparticles on the surface of the inorganic shell layer. The PDA/MCB coating allows MCB-MPCC to absorb sunlight over a wider wavelength range, resulting in higher light absorbance [125,126]. The n-docosane gives MCB-MPCC a high latent heat capacity of 145 J g⁻¹. The evaporation rate of MCB-MPCC can reach 2.67 kg m⁻² h⁻¹ under one sunlight intensity irradiation.

This part summarizes and analyses typical solar interface evaporators with phase change microcapsule structure. By encapsulating the PCM inside dense spheres, the issue of PCM leakage due to phase change melting can be better addressed. By applying a coating of photothermal conversion materials on the surface of the spheres, the photothermal conversion capability of the phase change microcapsules is enhanced, leading to improved utilization of solar energy. The performance of the evaporators designed with four different materials is summarized in Table 3. Compared to the others, MXene photothermal conversion material has the highest photothermal conversion efficiency. However, under the same light conditions, the evaporation rate of the MCB-MPCC evaporator is 2.67 kg m⁻² h⁻¹, which is higher than the other three evaporators. Comparative analysis of microcapsule-structured solar interfacial evaporators allows for a better comparison of the different properties brought about by different material designs, providing researchers with a wider range of options.

4. Conclusion and challenges

PCMs can effectively solve the problem of low efficiency of solar desalination system due to the intermittency and instability of solar energy. The study of PCMs is of great significance to improve the efficiency of solar desalination system. This paper focuses on a comprehensive analysis of the application of PCMs in two types of seawater evaporation systems, solar still and solar interface evaporator, and draws the following conclusions:

- (1) In solar still systems with integrated PCMs, the PCMs are mainly located at the bottom of basin as well as individually encapsulated in the basin. PW is the most commonly used PCM in solar stills. Its thermal conductivity can be improved by adding metal nanoparticles to facilitate heat transfer. In addition, through the structural design of the distiller and system integration, its evaporation performance and energy utilization are significantly improved. The improvement in evaporation performance is even

Table 3

Performance of solar interface evaporators with microencapsulated structures of different material designs.

Materials	Thermal conversion efficiency (%)	Eva-rate (kg·m ⁻² ·h ⁻¹)	Eva-efficiency (%)	Ref.
MoS ₂ -MEPCM	96.86 %	2.06	95.30 %	[117]
MXene/SA/-SiO ₂ -MEPCM	97.00 %	2.11	80.88 %	[121]
Cppy-O	96.00 %	2.62	92.70 %	[124]
MCB-MPCC	91.70 %	2.67	82.90 %	[95]

- more pronounced when solar stills are integrated with other systems.
- (2) To solve the problem of latent heat loss during condensation of vapour, the PCMs are combined with a heat pipe. The energy released from steam condensation is stored in the PCMs, released at night. It is also transferred to the seawater through the heat pipe, thus maintaining the continuous operation of the still. By combining an external condenser with PCMs for latent heat recovery, water production can be increased by 86 %. Latent heat recovery plays a vital role in improving the performance of the still.
 - (3) In the gel-structured solar interfacial evaporator, the gel serves as a support material for the whole evaporator and provides a stable place for PCMs. By adding the photo-thermal conversion material, a dual-function interfacial evaporator with both photo-thermal conversion and energy storage is formed. The performance of the evaporator depends on the selection of different composition structures, photothermal conversion materials and PCM. The BF/PVA/CB evaporator using graphene and PW as the solid-solid PCM exhibited a higher evaporation rate ($3.80 \text{ kg m}^{-2} \text{ h}^{-1}$) and evaporation efficiency (151 %) compared to other evaporators. This provides inspiration for researchers studying PCMs-integrated gel-structured solar interfacial evaporators, thus contributing to the further development of the field.
 - (4) The microcapsule-structured solar interface evaporator used a dense inorganic shell to wrap the PCM to solve the leakage problem. In order to enhance its photo-thermal conversion capability, a photo-thermal conversion material was applied as a coating on the outer surface of the shell. This coating is able to convert solar energy into thermal energy for water evaporation and thermal energy storage. Among the various photothermal conversion materials, MXene material has a high conversion efficiency of 97 % due to its characteristics. The combination of photothermal conversion materials with high photothermal conversion efficiency and PCMs with high energy storage density results in a microcapsule-structured interfacial evaporator with high evaporation rate and evaporation efficiency.
 - (5) Solar interfacial evaporators are more energy-efficient than solar stills. They only require heating of the seawater at the interface to cause evaporation. Additionally, the photo-thermal conversion materials used in solar interfacial evaporators have higher light absorption and photo-thermal conversion capacity. Solar distillers often require materials that can withstand high temperatures and vapour corrosion, resulting in higher manufacturing and maintenance costs. In contrast, solar interface evaporators have a simpler structure and lower manufacturing costs. Therefore, solar interfacial evaporators have become a research hotspot for solar desalination systems.
 - (6) The solar-powered desalination system that has been designed demonstrates a high removal rate for the four most common typical salt ions (K^+ , Ca^{2+} , Na^+ , and Mg^{2+}) found in water. Following the desalination process, the concentration of salt ions in the condensed water is greatly diminished and falls well below the drinking water standards established by the WHO. This indicates that the solar-powered interface evaporator has excellent salt filtration capabilities.

However, in order to advance solar-powered desalination technology, it still faces numerous challenges. There is still a considerable amount of research that remains to be undertaken, including but not limited to the following areas:

- (1) When the stored latent heat in the PCMs is used as the energy source for seawater evaporation, the evaporation rate is relatively low and the duration of evaporation is short. Therefore, further research is needed to increase the thermal energy storage

capacity to extend the operating time of the night evaporator and increase the night evaporation rate.

- (2) When the evaporator is used for seawater desalination, it does not cause salt accumulation behavior for a short period of time, and a small amount of accumulated salt will be removed automatically through the concentration difference. However, after the evaporator has operated for a long time, the accumulated salt gradually increases, which hinders the absorption of sunlight and reduces the evaporation performance of the evaporator. Therefore, it is of great significance to study how to enhance the self-purification ability of the evaporator for high concentration of salt to prolong the service life of the evaporator and improve its evaporation performance.

CRediT authorship contribution statement

Bing Xu: Writing – original draft, Visualization, Conceptualization. **Xiaoguang Zhao:** Software, Visualization. **Xiaochao Zuo:** Conceptualization, Supervision, Writing – review & editing. **Huaming Yang:** Conceptualization, Resources, Supervision, Writing – review & editing.

Declaration of competing interest

The authors declare that they have no known competing financial interests or personal relationships that could have appeared to influence the work reported in this paper.

Data availability

Data will be made available on request.

Acknowledgements

This work was supported by the National Key R&D Program of China (2022YFC2904802), the CUG Scholar Scientific Research Funds at China University of Geosciences (Wuhan) (2019152), the Fundamental Research Funds for the Central Universities at China University of Geosciences (Wuhan), and the National Science Fund for Distinguished Young Scholars (51225403).

References

- [1] M. Rousta, A. Kasaeian, A. Kouravand, G. Kasaeian, M.A. Vaziri Rad, Experimental investigation on tubular solar desalination using phase change material enhanced with nano- Co_3O_4 and aluminum shavings, Desalination 567 (2023) 116972.
- [2] M.W. Shahzad, M. Burhan, L. Ang, K.C. Ng, Energy-water-environment nexus underpinning future desalination sustainability, Desalination 413 (2017) 52–64.
- [3] Z. Li, X. Xu, X. Sheng, P. Lin, J. Tang, L. Pan, Y.V. Kaneti, T. Yang, Y. Yamauchi, Solar-powered sustainable water production: state-of-the-art technologies for sunlight–energy–water nexus, ACS Nano 15 (2021) 12535–12566.
- [4] Z.M. Omara, A.E. Kabeel, A.S. Abdullah, A review of solar still performance with reflectors, Renew. Sustain. Energy Rev. 68 (2017) 638–649.
- [5] S.W. Sharshir, A.H. Elsheikh, G. Peng, N. Yang, M.O.A. El-Samadony, A.E. Kabeel, Thermal performance and exergy analysis of solar stills – a review, Renew. Sustain. Energy Rev. 73 (2017) 521–544.
- [6] A. Shahsavari, M. Afrand, R. Kalbasi, S. Aghakhani, H.R. Bakhtsheshi-Rad, N. Karimi, A comprehensive review on the application of nanofluids and PCMs in solar thermal collectors: energy, exergy, economic, and environmental analyses, J. Taiwan Inst. Chem. Eng. 148 (2023) 104856.
- [7] S. Manju, N. Nagar, Renewable energy integrated desalination: a sustainable solution to overcome future fresh-water scarcity in India, Renew. Sustain. Energy Rev. 73 (2017) 594–609.
- [8] A. El Fadar, Novel process for performance enhancement of a solar continuous adsorption cooling system, Energy 114 (2016) 10–23.
- [9] M. Edalatpour, K. Aryana, A. Kianifar, G.N. Tiwari, O. Mahian, S. Wongwises, Solar stills: a review of the latest developments in numerical simulations, Sol. Energy 135 (2016) 897–922.
- [10] D. Dsilva Winfred Rufuss, S. Injyan, L. Suganthi, P.A. Davies, Solar stills: a comprehensive review of designs, performance and material advances, Renew. Sustain. Energy Rev. 63 (2016) 464–496.

- [11] L. Li, J. Zhang, Highly salt-resistant and all-weather solar-driven interfacial evaporators with photothermal and electrothermal effects based on Janus graphene@silicone sponges, *Nano Energy* 81 (2021) 105682.
- [12] Y. Guo, Y. Sui, J. Zhang, Z. Cai, B. Xu, An all-day solar-driven vapor generator via photothermal and Joule-heating effects, *J. Mater. Chem. A* 8 (2020) 25178–25186.
- [13] P. Mu, L. Song, L. Geng, J. Li, Aligned Attapulgite-based aerogels with excellent mechanical property for the highly efficient solar steam generation, *Sep. Purif. Technol.* 271 (2021) 118869.
- [14] F.L. Meng, M. Gao, T. Ding, G. Yilmaz, W.L. Ong, G.W. Ho, Modular deformable steam electricity cogeneration system with photothermal, water, and electrochemical tunable multilayers, *Adv. Funct. Mater.* 30 (2020) 2002867.
- [15] W. Xu, X. Hu, S. Zhuang, Y. Wang, X. Li, L. Zhou, S. Zhu, J. Zhu, Flexible and salt resistant janus absorbers by electrospinning for stable and efficient solar desalination, *Adv. Energy Mater.* 8 (2018) 1702884.
- [16] B. Saleh, F.A. Essa, A. Aly, M. Alsehli, H. Panchal, A. Afzal, S. Shamugan, Investigating the performance of dish solar distiller with phase change material mixed with Al_2O_3 nanoparticles under different water depths, *Environ. Sci. Pollut. Control Ser.* 29 (2022) 28115–28126.
- [17] H. Panchal, K. Patel, M. Elkelawy, H.A.-E. Bastawissi, A use of various phase change materials on the performance of solar still: a review, *Int. J. Ambient Energy* 42 (2019) 1575–1580.
- [18] H. Yi, L. Xia, S. Song, Three-dimensional montmorillonite/Ag nanowire aerogel supported stearic acid as composite phase change materials for superior solar-thermal energy harvesting and storage, *Compos. Sci. Technol.* 217 (2022) 109121.
- [19] H. Yi, Z. Ai, Y. Zhao, X. Zhang, S. Song, Design of 3D-network montmorillonite nanosheet/stearic acid shape-stabilized phase change materials for solar energy storage, *Sol. Energy Mater. Sol. Cell.* 204 (2020) 110233.
- [20] F.S. Javadi, H.S.C. Metselaar, P. Ganeshan, Performance improvement of solar thermal systems integrated with phase change materials (PCM), a review, *Sol. Energy* 206 (2020) 330–352.
- [21] X. Du, J. Qiu, S. Deng, Z. Du, X. Cheng, H. Wang, Flame-retardant and solid-solid phase change composites based on dopamine-decorated BP nanosheets/Polyurethane for efficient solar-to-thermal energy storage, *Renew. Energy* 164 (2021) 1–10.
- [22] T. Saito, S. Brown, S. Chatterjee, J. Kim, C. Tsouris, R.T. Mayes, L.-J. Kuo, G. Gill, Y. Oyola, C.J. Janke, S. Dai, Uranium recovery from seawater: development of fiber adsorbents prepared via atom-transfer radical polymerization, *J. Mater. Chem. A* 2 (2014) 14674–14681.
- [23] M. Shatat, S. Riffat, G. Gan, An innovative psychometric solar-powered water desalination system, *Int. J. Low Carbon Technol.* 11 (2016) 254–265.
- [24] H.E.S. Fath, Solar distillation: a promising alternative for water provision with free energy, simple technology and a clean environment, *Desalination* 116 (1998) 45–56.
- [25] F.F. Tabrizi, M. Dashtban, H. Moghaddam, Experimental investigation of a weir-type cascade solar still with built-in latent heat thermal energy storage system, *Desalination* 260 (2010) 248–253.
- [26] N.K. Dhiman, Transient analysis of a spherical solar still, *Desalination* 69 (1988) 47–55.
- [27] Z.M. Omara, M.H. Hamed, A.E. Kabeel, Performance of finned and corrugated absorbers solar stills under Egyptian conditions, *Desalination* 277 (2011) 281–287.
- [28] H.R. Goshayeshi, M.R. Safaei, Effect of absorber plate surface shape and glass cover inclination angle on the performance of a passive solar still, *Int. J. Numer. Methods Heat Fluid Flow* 30 (2019) 3183–3198.
- [29] S.W. Sharshir, N. Yang, G. Peng, A.E. Kabeel, Factors affecting solar stills productivity and improvement techniques: a detailed review, *Appl. Therm. Eng.* 100 (2016) 267–284.
- [30] S.M. Shalaby, E. El-Bialy, A.A. El-Sebaii, An experimental investigation of a v-corrugated absorber single-basin solar still using PCM, *Desalination* 398 (2016) 247–255.
- [31] H. Mousa, A.M. Gujarathi, Modeling and analysis the productivity of solar desalination units with phase change materials, *Renew. Energy* 95 (2016) 225–232.
- [32] Y. Wang, J. Nie, Z. He, Y. Zhi, X. Ma, P. Zhong, $\text{Ti}_3\text{C}_2\text{Tx}$ MXene nanoflakes embedded with copper indium selenide nanoparticles for desalination and water purification through high-efficiency solar-driven membrane evaporation, *ACS Appl. Mater. Interfaces* 14 (2022) 5876–5886.
- [33] A.E. Kabeel, M. Abdelgaid, A. Eisa, Effect of graphite mass concentrations in a mixture of graphite nanoparticles and paraffin wax as hybrid storage materials on performances of solar still, *Renew. Energy* 132 (2019) 119–128.
- [34] V.S. Reddy, S.C. Kaushik, S.K. Tyagi, Exergetic analysis and performance evaluation of parabolic trough concentrating solar thermal power plant (PTCSTPP), *Energy* 39 (2012) 258–273.
- [35] G.N. Tiwari, L. Sahota, Review on the energy and economic efficiencies of passive and active solar distillation systems, *Desalination* 401 (2017) 151–179.
- [36] G.N. Tiwari, V. Dimri, A. Chel, Parametric study of an active and passive solar distillation system: energy and exergy analysis, *Desalination* 242 (2009) 1–18.
- [37] V.K. Dwivedi, G.N. Tiwari, Experimental validation of thermal model of a double slope active solar still under natural circulation mode, *Desalination* 250 (2010) 49–55.
- [38] M. Asbil, H. Boushaba, H. Hafs, A. Koukouch, A. Sabri, A. Muthu Manokar, Investigating the effect of sensible and latent heat storage materials on the performance of a single basin solar still during winter days, *J. Energy Storage* 44 (2021) 103480.
- [39] J. Kateshia, V.J. Lakhera, Analysis of solar still integrated with phase change material and pin fins as absorbing material, *J. Energy Storage* 35 (2021) 102292.
- [40] A.E. Kabeel, M. Elkelawy, H. Alm El Din, A. Alghrubah, Investigation of exergy and yield of a passive solar water desalination system with a parabolic concentrator incorporated with latent heat storage medium, *Energy Convers. Manag.* 145 (2017) 10–19.
- [41] R. Sathyamurthy, S.A. El-Agouz, P.K. Nagarajan, J. Subramani, T. Arunkumar, D. Mageshbabu, B. Madhu, R. Bharathwaaj, N. Prakash, A Review of integrating solar collectors to solar still, *Renew. Sustain. Energy Rev.* 77 (2017) 1069–1097.
- [42] A.E. Kabeel, R. Sathyamurthy, A.M. Manokar, S.W. Sharshir, F.A. Essa, A. H. Elshiekh, Experimental study on tubular solar still using Graphene Oxide Nano particles in Phase Change Material (NPCM's) for fresh water production, *J. Energy Storage* 28 (2020) 101204.
- [43] A. Shukla, K. Kant, A. Sharma, Solar still with latent heat energy storage: a review, *Innovat. Food Sci. Emerg. Technol.* 41 (2017) 34–46.
- [44] V.S. Vigneswaran, G. Kumaresan, B.V. Dinakar, K.K. Kamal, R. Velraj, Augmenting the productivity of solar still using multiple PCMs as heat energy storage, *J. Energy Storage* 26 (2019) 101019.
- [45] V.K. Chauhan, S.K. Shukla, P.K.S. Rathore, A systematic review for performance augmentation of solar still with heat storage materials: a state of art, *J. Energy Storage* 47 (2022) 103578.
- [46] J. Mustafa, S. Alqaed, M. Sharifpur, Two phase simulation of solar still in the presence of phase change materials in its bottom and aluminum nanoparticles in the water, *Case Stud. Therm. Eng.* 49 (2023) 103357.
- [47] A.J. Chamka, D.W. Rufuss, A.E. Kabeel, R. Sathyamurthy, M. Abdelgaid, A. M. Manokar, B. Madhu, Augmenting the potable water produced from single slope solar still using CNT-doped paraffin wax as energy storage: an experimental approach, *J. Braz. Soc. Mech. Eng.* 42 (2020) 625.
- [48] M. Sheikholeslami, Modeling investigation for energy storage system including mixture of paraffin and ZnO nano-powders considering porous media, *J. Petrol. Sci. Eng.* 219 (2022) 111066.
- [49] M.J. Alshukri, A.A. Eidan, S.I. Najim, The influence of integrated Micro-ZnO and Nano-CuO particles/paraffin wax as a thermal booster on the performance of heat pipe evacuated solar tube collector, *J. Energy Storage* 37 (2021) 102506.
- [50] P.M. Kumar, K. Mysamy, A comprehensive study on thermal storage characteristics of nano- CeO_2 embedded phase change material and its influence on the performance of evacuated tube solar water heater, *Renew. Energy* 162 (2020) 662–676.
- [51] A.V. Arasu, A.P. Sasmito, A.S. Mujumdar, Thermal performance enhancement of paraffin wax with Al_2O_3 and CuO nanoparticles-A numerical study, *Frontiers in Heat and Mass Transfer* 2 (2012) 043005.
- [52] P. B. V. A., Stability analysis of $\text{TiO}_2\text{-Ag}$ nanocomposite particles dispersed paraffin wax as energy storage material for solar thermal systems, *Renew. Energy* 152 (2020) 358–367.
- [53] S.S. Adibi Toosi, H.R. Goshayeshi, I. Zahmatkesh, V. Nejati, Experimental assessment of new designed stepped solar still with Fe_3O_4 +graphene oxide+paraffin as nanofluid under constant magnetic field, *J. Energy Storage* 62 (2023) 106795.
- [54] R. Sathyamurthy, Silver (Ag) based nanoparticles in paraffin wax as thermal energy storage for stepped solar still-An experimental approach, *Sol. Energy* 262 (2023) 111808.
- [55] A.E. Kabeel, M.A. Teamah, M. Abdelgaid, G.B. Abdel Aziz, Modified pyramid solar still with v-corrugated absorber plate and PCM as a thermal storage medium, *J. Clean. Prod.* 161 (2017) 881–887.
- [56] A.S. Abdullah, Z.M. Omara, H.B. Bacha, M.M. Younes, Employing convex shape absorber for enhancing the performance of solar still desalination system, *J. Energy Storage* 47 (2022) 103573.
- [57] M. Afrand, R. Kalbasi, A. Karimpour, S. Wongwises, Experimental investigation on a thermal model for a basin solar still with an external reflector, *Energies* 10 (2017) 18.
- [58] S. Maiti, C. Bhatt, P. Patel, P.K. Ghosh, Practical and sustainable household seawater desalination using an improved solar still, *Desalination Water Treat.* 57 (2014) 3358–3371.
- [59] F.A. Essa, A.S. Abdullah, Z.M. Omara, A.E. Kabeel, Y. Gamiel, Experimental study on the performance of trays solar still with cracks and reflectors, *Appl. Therm. Eng.* 188 (2021) 116652.
- [60] S. Shoeibi, H. Kargarsharifabadi, S.A.A. Mirjalili, T. Muhammad, Solar district heating with solar desalination using energy storage material for domestic hot water and drinking water-Environmental and economic analysis, *Sustain. Energy Technol. Assessments* 49 (2022) 101713.
- [61] S. Shoeibi, H. Kargarsharifabadi, N. Rahbar, Effects of nano-enhanced phase change material and nano-coated on the performance of solar stills, *J. Energy Storage* 42 (2021) 103061.
- [62] D. Sathish, S. Jegadheeswaran, M. Veeramanikandan, Enhancing the thermo-economic performance of mobile solar desalination system with dual reflectors, phase change materials and insulator cover: experimental investigations, *Appl. Therm. Eng.* 217 (2022) 119210.
- [63] K. Sampathkumar, T.V. Arjunan, P. Pitchandi, P. Senthilkumar, Active solar distillation-A detailed review, *Renew. Sustain. Energy Rev.* 14 (2010) 1503–1526.
- [64] F. Trieb, H. Müller-Steinhagen, J. Kern, J. Scharfe, M. Kabariti, A. Al Taher, Technologies for large scale seawater desalination using concentrated solar radiation, *Desalination* 235 (2009) 33–43.
- [65] K. Sampathkumar, P. Senthilkumar, Utilization of solar water heater in a single basin solar still-An experimental study, *Desalination* 297 (2012) 8–19.

- [66] N. Joy, A. Antony, A. Anderson, Experimental study on improving the performance of solar still using air blower, *Int. J. Ambient Energy* 39 (2017) 613–616.
- [67] S.A. El-Agouz, Experimental investigation of stepped solar still with continuous water circulation, *Energy Convers. Manag.* 86 (2014) 186–193.
- [68] A.E. Kabeel, M. Abdelgaiad, M. Mahgoub, The performance of a modified solar still using hot air injection and PCM, *Desalination* 379 (2016) 102–107.
- [69] A.E. Kabeel, M.M. Khairat Dawood, K. Ramzy, T. Nabil, B. Elnaghi, A. elkassar, Enhancement of single solar still integrated with solar dishes: an experimental approach, *Energy Convers. Manag.* 196 (2019) 165–174.
- [70] N. Wang, D. Wang, J. Dong, H. Wang, R. Wang, L. Shao, Y. Zhu, Performance assessment of PCM-based solar energy assisted desiccant air conditioning system combined with a humidification-dehumidification desalination unit, *Desalination* 496 (2020) 114705.
- [71] A.I. Shehata, A.E. Kabeel, M.M. Khairat Dawood, A.M. Elharidi, A. Abd Elsalam, K. Ramzy, A. Mehanna, Enhancement of the productivity for single solar still with ultrasonic humidifier combined with evacuated solar collector: an experimental study, *Energy Convers. Manag.* 208 (2020) 112592.
- [72] A.K. Thakur, R. Sathyamurthy, R. Velraj, Development of candle soot dispersed phase change material for improving water generation potential of tubular solar distillation unit, *Sol. Energy Mater. Sol. Cell.* 241 (2022) 111748.
- [73] T. Arunkumar, D. Denkenberger, R. Velraj, R. Sathyamurthy, H. Tanaka, K. Vinothkumar, Experimental study on a parabolic concentrator assisted solar desalting system, *Energy Convers. Manag.* 105 (2015) 665–674.
- [74] Z.Y. Ho, R. Bahar, C.H. Koo, Passive solar stills coupled with Fresnel lens and phase change material for sustainable solar desalination in the tropics, *J. Clean. Prod.* 334 (2022) 130279.
- [75] M. Elashmawy, M. Alhadri, M.M.Z. Ahmed, Enhancing tubular solar still performance using novel PCM-tubes, *Desalination* 500 (2021) 114880.
- [76] B. Thamarai Kannan, B. Madhu, A.E. Kabeel, A.K. Thakur, R. Velraj, I. Lynch, R. Saidur, R. Sathyamurthy, Improved freshwater generation via hemispherical solar desalination unit using paraffin wax as phase change material encapsulated in waste aluminium cans, *Desalination* 538 (2022) 115907.
- [77] A. Kaabinejadian, M. Moghimi, I. Fakhari, Design, modeling, and thermo-economic optimization of an innovative continuous solar-powered hybrid desalination plant integrated with latent heat thermal energy storage, *Appl. Therm. Eng.* 219 (2023) 119576.
- [78] H. Ami Ahmadni, N. Varjji, A. Kaabinejadian, M. Moghimi, M. Siavashi, Optimal design and sensitivity analysis of energy storage for concentrated solar power plants using phase change material by gradient metal foams, *J. Energy Storage* 35 (2021) 102233.
- [79] K.Y. Leong, M.R. Abdul Rahman, B.A. Gurunathan, Nano-enhanced phase change materials: a review of thermo-physical properties, applications and challenges, *J. Energy Storage* 21 (2019) 18–31.
- [80] A. Madhlopa, C. Johnstone, Numerical study of a passive solar still with separate condenser, *Renew. Energy* 34 (2009) 1668–1677.
- [81] P. Monowe, M. Masale, N. Nijegorodov, V. Vasilenko, A portable single-basin solar still with an external reflecting booster and an outside condenser, *Desalination* 280 (2011) 332–338.
- [82] M.B. Shafii, M. Shahmohamadi, M. Faegh, H. Sadroosseini, Examination of a novel solar still equipped with evacuated tube collectors and thermoelectric modules, *Desalination* 382 (2016) 21–27.
- [83] M. Faegh, M.B. Shafii, Experimental investigation of a solar still equipped with an external heat storage system using phase change materials and heat pipes, *Desalination* 409 (2017) 128–135.
- [84] P. Zhang, J. Li, L. Lv, Y. Zhao, L. Qu, Vertically aligned graphene sheets membrane for highly efficient solar thermal generation of clean water, *ACS Nano* 11 (2017) 5087–5093.
- [85] S. Zhuang, L. Zhou, W. Xu, N. Xu, X. Hu, X. Li, G. Lv, Q. Zheng, S. Zhu, Z. Wang, J. Zhu, Tuning transpiration by interfacial solar absorber-leaf engineering, *Adv. Sci.* 5 (2017) 1700497.
- [86] Z. Huang, S. Li, X. Cui, Y. Wan, Y. Xiao, S. Tian, H. Wang, X. Li, Q. Zhao, C.-S. Lee, A broadband aggregation-independent plasmonic absorber for highly efficient solar steam generation, *J. Mater. Chem. A* 8 (2020) 10742–10746.
- [87] Q. Huang, X. Liang, C. Yan, Y. Liu, Review of interface solar-driven steam generation systems: high-efficiency strategies, applications and challenges, *Appl. Energy* 283 (2021) 116361.
- [88] A.H. Elsheikh, S.W. Sharshir, M.K. Ahmed Ali, J. Shaibo, E.M.A. Edreis, T. Abdelhamid, C. Du, Z. Haiou, Thin film technology for solar steam generation: a new dawn, *Sol. Energy* 177 (2019) 561–575.
- [89] P.-F. Liu, L. Miao, Z. Deng, J. Zhou, Y. Gu, S. Chen, H. Cai, L. Sun, S. Tanemura, Flame-treated and fast-assembled foam system for direct solar steam generation and non-plugging high salinity desalination with self-cleaning effect, *Appl. Energy* 241 (2019) 652–659.
- [90] L. Zhu, M. Gao, C.K.N. Peh, G.W. Ho, Recent progress in solar-driven interfacial water evaporation: advanced designs and applications, *Nano Energy* 57 (2019) 507–518.
- [91] S. Liu, C. Huang, X. Luo, C. Guo, Performance optimization of bi-layer solar steam generation system through tuning porosity of bottom layer, *Appl. Energy* 239 (2019) 504–513.
- [92] J. Yan, Q. Wu, J. Wang, W. Xiao, G. Zhang, H. Xue, J. Gao, Carbon nanofiber reinforced carbon aerogels for steam generation: synergy of solar driven interface evaporation and side wall induced natural evaporation, *J. Colloid Interface Sci.* 641 (2023) 1033–1042.
- [93] H. Liu, D. Tian, Z. Zheng, X. Wang, Z. Qian, MXene-decorated magnetic phase-change microcapsules for solar-driven continuous seawater desalination with easy salt accumulation elimination, *Chem. Eng. J.* 458 (2023) 141395.
- [94] J. Zhou, L. Yang, X. Cao, Y. Ma, H. Sun, J. Li, Z. Zhu, R. Jiao, W. Liang, A. Li, MXene nanosheets coated conjugated microporous polymers hollow microspheres incorporating with phase change material for continuous desalination, *J. Colloid Interface Sci.* 654 (2024) 819–829.
- [95] W. Li, Z. Zheng, H. Liu, X. Wang, A solar-driven seawater desalination and electricity generation integrating system based on carbon black-decorated magnetic phase-change composites, *Desalination* 562 (2023) 116713.
- [96] Y. Tian, H. Yang, S. Wu, J. Yan, K. Cen, T. Luo, G. Xiong, Y. Hou, Z. Bo, K. Ostrikov, Beyond lotus: plasma nanostructuring enables efficient energy and water conversion and use, *Nano Energy* 66 (2019) 104125.
- [97] Y. Shi, R. Li, Y. Jin, S. Zhuo, L. Shi, J. Chang, S. Hong, K.-C. Ng, P. Wang, A 3D photothermal structure toward improved energy efficiency in solar steam generation, *Joule* 2 (2018) 1171–1186.
- [98] J. Li, X. Wang, Z. Lin, N. Xu, X. Li, J. Liang, W. Zhao, R. Lin, B. Zhu, G. Liu, L. Zhou, S. Zhu, J. Zhu, Over 10 kg m⁻² h⁻¹ evaporation rate enabled by a 3D interconnected porous carbon foam, *Joule* 4 (2020) 928–937.
- [99] B. Gong, H. Yang, S. Wu, Y. Tian, J. Yan, K. Cen, Z. Bo, K. Ostrikov, Phase change material enhanced sustained and energy-efficient solar-thermal water desalination, *Appl. Energy* 301 (2021) 117463.
- [100] A. Sari, A. Biger, C. Alkan, Thermal energy storage properties of polyethylene glycol grafted styrene copolymer as novel solid-solid phase change materials, *Int. J. Energy Res.* 44 (2020) 3976–3989.
- [101] F. Xue, Y. Lu, X.-d. Qi, J.-h. Yang, Y. Wang, Melamine foam-templated graphene nanoplatelet framework toward phase change materials with multiple energy conversion abilities, *Chem. Eng. J.* 365 (2019) 20–29.
- [102] Y. Wu, L. Shen, C. Zhang, H. Gao, J. Chen, L. Jin, P. Lin, H. Zhang, Y. Xia, Polyacid doping-enabled efficient solar evaporation of polypyrrole hydrogel, *Desalination* 505 (2021) 114766.
- [103] Y.-w. Shao, W.-w. Hu, M.-h. Gao, Y.-y. Xiao, T. Huang, N. Zhang, J.-h. Yang, X.-d. Qi, Y. Wang, Flexible MXene-coated melamine foam based phase change material composites for integrated solar-thermal energy conversion/storage, shape memory and thermal therapy functions, *Compos. Appl. Sci. Manuf.* 143 (2021) 106291.
- [104] X. Zhao, X. Zuo, H. Yang, Advances in nanoclay-based form stable phase change materials: a review, *Advanced Materials Technologies* 8 (2023) 2300961.
- [105] X. Zuo, X. Zhang, Y. Tang, Y. Zhang, X. Li, H. Yang, Preparation of serpentine fiber/poly (vinyl alcohol) aerogel with high compressive strength to stabilize phase change materials for thermal energy storage, *Appl. Clay Sci.* 247 (2024) 107214.
- [106] Z. Zheng, H. Liu, D. Wu, X. Wang, Polyimide/MXene hybrid aerogel-based phase-change composites for solar-driven seawater desalination, *Chem. Eng. J.* 440 (2022) 135862.
- [107] Q. Guo, H. Yi, F. Jia, S. Song, Design of MoS₂/MMT bi-layered aerogels integrated with phase change materials for sustained and efficient solar desalination, *Desalination* 541 (2022) 116028.
- [108] F. Yu, Z. Guo, Y. Xu, Z. Chen, M.S. Irshad, J. Qian, T. Mei, X. Wang, Biomass-derived bilayer solar evaporator with enhanced energy utilization for high-efficiency water generation, *ACS Appl. Mater. Interfaces* 12 (2020) 57155–57164.
- [109] Y. Liang, J. Guo, J.J. Li, J. Mao, A.Q. Xie, L. Zhu, S. Chen, Robust and flexible 3D photothermal evaporator with heat storage for high-performance solar-driven evaporation, *Advanced Sustainable Systems* 6 (2022) 2200236.
- [110] H. Deng, Y. Yang, X. Tang, Y. Li, F. He, Q. Zhang, Z. Huang, Z. Yang, W. Yang, Phase-change composites composed of silicone rubber and Pa@SiO₂@PDA double-shelled microcapsules with low leakage rate and improved mechanical strength, *ACS Appl. Mater. Interfaces* 13 (2021) 39394–39403.
- [111] A. Zhao, J. An, J. Yang, E.-H. Yang, Microencapsulated phase change materials with composite titania-polyurea (TiO₂-PUA) shell, *Appl. Energy* 215 (2018) 468–478.
- [112] T. Wang, S. Wang, R. Luo, C. Zhu, T. Akiyama, Z. Zhang, Microencapsulation of phase change materials with binary cores and calcium carbonate shell for thermal energy storage, *Appl. Energy* 171 (2016) 113–119.
- [113] X. Chen, Z. Tang, P. Liu, H. Gao, Y. Chang, G. Wang, Smart utilization of multifunctional metal oxides in phase change materials, *Matter* 3 (2020) 708–741.
- [114] Y. Wuliu, J. Liu, L. Zhang, S. Wang, Y. Liu, J. Feng, X. Liu, Design of bio-based organic phase change materials containing a “safety valve”, *Green Chem.* 23 (2021) 8643–8656.
- [115] S. Zhao, A. Yuan, H. Xu, Z. Wei, S. Zhou, Y. Xiao, L. Jiang, J. Lei, Elevating the photothermal conversion efficiency of phase-change materials simultaneously toward solar energy storage, self-healing, and recyclability, *ACS Appl. Mater. Interfaces* 14 (2022) 29213–29222.
- [116] D. Li, X. Zuo, X. Zhang, Y. Tang, X. Zhao, Y. Zhang, H. Yang, Emerging urchin-like core-shell mineral microspheres with efficient photothermal conversion and solar energy storage, *J. Energy Storage* 68 (2023) 107661.
- [117] H. Shen, Z. Zheng, H. Liu, X. Wang, A solar-powered interfacial evaporation system based on MoS₂-decorated magnetic phase-change microcapsules for sustainable seawater desalination, *J. Mater. Chem. A* 10 (2022) 25509–25526.
- [118] Y. Peng, S. Tang, X. Wang, R. Ran, A high strength hydrogel with a core-shell structure simultaneously serving as strain sensor and solar water evaporator, *Macromol. Mater. Eng.* 306 (2021) 2100309.
- [119] A. Alrasheed, J.M. Gorham, B.C. Tran Khac, F. Alsaffar, F.W. DelRio, K.-H. Chung, M.R. Amer, Surface properties of laser-treated molybdenum disulfide nanosheets

- for optoelectronic applications, *ACS Appl. Mater. Interfaces* 10 (2018) 18104–18112.
- [120] P. Lin, J. Xie, Y. He, X. Lu, W. Li, J. Fang, S. Yan, L. Zhang, X. Sheng, Y. Chen, MXene aerogel-based phase change materials toward solar energy conversion, *Sol. Energy Mater. Sol. Cell.* 206 (2020).
- [121] M. Zhang, K. Sun, Z. Zheng, H. Liu, X. Wang, Development of MXene-decorated sodium alginate/SiO₂@n-docosane hierarchical phase-change microcapsules for solar-driven sustainable seawater desalination, *Desalination* 550 (2023) 116380.
- [122] C. Liu, Y. Peng, X. Zhao, Flower-inspired bionic sodium alginate hydrogel evaporator enhancing solar desalination performance, *Carbohydr. Polym.* 273 (2021) 118536.
- [123] Z. Ai, Y. Zhao, R. Gao, L. Chen, T. Wen, W. Wang, T. Zhang, W. Ge, S. Song, Self-assembly hierarchical binary gel based on MXene and montmorillonite nanosheets for efficient and stable solar steam generation, *J. Clean. Prod.* 357 (2022) 132000.
- [124] L. Geng, L. Li, H. Zhang, M. Zhong, P. Mu, J. Li, Interfacial solar evaporator synergistic phase change energy storage for all-day steam generation, *J. Mater. Chem. A* 10 (2022) 15485–15496.
- [125] S. Jiao, M. Liu, Y. Li, H. Abrha, J. Wang, Y. Dai, J. Li, N. Kang, Y. Li, X. Liu, Emerging hydrovoltaic technology based on carbon black and porous carbon materials: a mini review, *Carbon* 193 (2022) 339–355.
- [126] H. Gao, Y. Sun, J. Zhou, R. Xu, H. Duan, Mussel-Inspired synthesis of polydopamine-functionalized graphene hydrogel as reusable adsorbents for water purification, *ACS Appl. Mater. Interfaces* 5 (2013) 425–432.